TRANSPORT PHENOMENON OF PHOTO INJECTED ELECTRONS IN DYE SENSITIZED SOLAR CELLS.

BY:

KAHUTHU STANLEY WAMBUGU

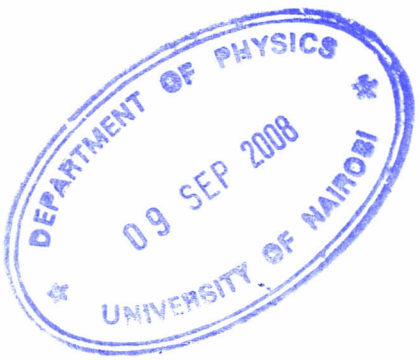

THIS PROJECT REPORT IS SUBMITTED AS PARTIAL FULFILMENT FOR THE DEGREE OF MASTER OF SCIENCE IN PHYSICS OF UNIVERSITY OF NAIROBI.

AUGUST 2008.

DECLARATION

This project report is my own work and has not been presented for a degree in any other university.

Kahuthu Stanley Wambugu

Signature ..... Date 17/09/2008

This project has been submitted for examination with the approval of my university supervisors:

Dr. L. Gwaki

Signature ..... Date 17/09/08

Dr. J. M. Mwabora

Signature ..... Date 17/09/08

Department of Physics,
University of Nairobi,
Nairobi, Kenya.

ACKNOWLEDGEMENT

I would like to express my heart felt gratitude to my supervisors, Dr. Lino and Dr. Mwabora, for their tireless effort that they made to ensure that my research work has taken the right direction by consistently guiding me through out from my initial step to the end.

I would also like to sincerely thank Mr. Musembi and Mr. Waita for their great concern in my research work and particularly ensuring that I was always in touch with the most recent scientific papers and even providing those scientific journals that they felt that they were of great use to me especially in my project work.

I would also express my thank to Dr. Kaduki, the chairman of department of physics, who ensured that after every three month I had to present a progress report to the department of Physics of University of Nairobi.

My sincere thanks go to the entire staff, both teaching and supportive, who have made available all kinds of technical help to ensure that I succeeded in this research work.

TABLE OF CONTENT

CHAPTER 4

CHAPTER 5

EFFECT OF TEMPERATURE ON DSSCs

CHAPTER 6

List of Abbreviations.

AM	Air Mass.
BP, BGR	British Petroleum
CB	Conduction Band.
CT	Charge Transfer.
DSSCs	Dye Sensitized Solar Cells.
D_{ox}	Density of empty states.
D_{red}	Density of occupied states.
EHPs	Electron Hole Pairs.
EIS	Electrochemical Impedance Spectroscopy.
IPCE	Incident Photon-to – Current Conversion Efficiency.
LHE	Light Harvest Efficiency.
TCO	Transparent Conducting Oxide.

Glossary of symbols.

A Cross-section area (cm^2), active area (cm^2) or a contant.
c Speed of electromagnetic radiation (3.0×10^8 m/ s^2).
D_n Electron diffusion constant (cm^{-3}).
D_p Hole diffusion constant (cm^{-3}).
E Electric field.
E_c ,E_v Conduction band and valence band energy respectively (J, eV)
E_F quasi Fermi energy (J, eV).
E_{Fn} , E_{Fp} Fermi level on n-side and p-side respectively.
E_g , Ego Energy gap and energy gap at 0K.
F Faraday constant
FF Fill Factor (dimensionless).
g, g_{th}, g_{op} Electron Hole Pair generation rate, thermally generation rate and optical generation rate respectively ($cm^{-3} - s^{-1}$).
h Planck's constant (6.63×10^{-34} J-s, eV-s).
$h\upsilon$ Photon energy (J , eV).
i, I Current (A).
I^-/ I_3^- Iodide/ triiodide
I_O Incident photon beam (photons/ cm^2 – s).
I_o Diode saturation current (A)
I_{op} Optically generated current (A)
I_D Diode current (A)
I_{diff} Diffusion current (A)
I_{max} Maximum current that correspond to the maximum power (A)
i_o Exchange current (A)
I_{ph} /I_L Photogenerated and light generated current (A)
I_{sc} Short circuit current (A)
I_{sh} Current flowing through shunt resistor (A)
I_{th} Thermal generated current (A)
K Kelvin
k Boltzmann constant (1.38×10^{-23} J/ K, eV / K)
LCA Life Cycle Assessment (dimensionless)

L_n / L_p Electron / Hole diffusion length (cm)
m Stoichiometric number of electrons involved in the electrode reaction.
m An integer (constant)
m_o Electronic rest mass (9.11×10^{-31}Kg)
n Ideality factor (dimensionless)
n n-type semiconductor material.
n concentration of electron in the conduction band (cm^{-3})
N_c effective density of states in the conduction band (m^{-3})
N_d concentration of donors (cm^2)
N_D,N_A concentration of ionised donors, acceptors
n_i intrinsic concentration (cm^{-3})
n_n, n_p equilibrium concentration of electrons in n-type and p-type material (cm^{-3})
η efficiency (dimensionless)
$\bar{n}$ equilibrium concentration in the n-type material under the influence of radiation (cm^{-3})
N_v effective density of states in the valence band (cm^{-3})
p p-type semiconductor material τ
p concentration of holes in the valence band (cm^{-3})
P_{max} maximum possible power from a given cell.
P_{in} total power in the light incident on the cell (W, mW)
p_n , p_p equilibrium concentration of holes in n-type and p-type material (cm^{-3})
$\bar{p}$, p_o equilibrium concentration under the radiation, thermal equilibrium concentration
P(V) Power out put as a function of Voltage.
q electronic charge (1.6×10^{-19} C)
R gas constant
R_1, R_2, R_3 Resistors numbered 1,2 and 3 respectively (ohms).
R_h Sheet resistance of Transparent Conducting Oxide (ohms cm^{-2})
R_L Load resistance (ohms)
R_s ,R_{sh} Series and shunt resistance respectively (ohms)
T absolute temperature (K)
V,U Voltage (V)
V_f forward bias voltage (V)
V_{max} maximum voltage (V)
V_o contact voltage (V)
V_{oc}, VOC open circuit voltage (V)
V_r reverse bias voltage (V)
W depletion region width (cm)
x_n,x_p distance in the neutral n-region and p-region of a junction measured from the edge of the transition region (cm)
x_{no} , x_{po} penetration of the transition region into n-region and p-region measured from metallurgical junction (cm)
Z_1 , Z_2, Z_3 Impedance due to capacitor 1,2 and 3 respectively (F)
υ frequency of electromagnetic radiation (Hz)
λ wave length (m) τ_p , τ_n hole and electron life time(s)
α optical absorption coefficient (cm^{-1})
δ_n , δ_p excess electron and hole, hole concentration (cm^{-3})

ABSTRACT

Transport phenomenon of photo injected electrons in Dye Sensitized Solar Cells (DSSC) has been studied and reported whereby the movement of charge carriers has been assumed to be predominantly by diffusion. A theoretical model was developed to study the effects of temperature on solar cell parameters. Based on the research paper by Koide et al.(2006) which clearly shows that the conventional solar cells equations are also applicable to Dye Sensitized Solar Cells (DSSC), explicit and implicit equations were developed that relate Open Circuit Voltage, V_{oc}, and Short Circuit Current, I_{sc}, respectively with the temperature, T, within the range 25^{o} (298K) $\leq T \leq 55^{o}$ (328K). Optoelectronic properties such as Efficiency, Fill Factor (FF) and Maximum Power Output ($P_{max.}$) were found to depend on the V_{oc}.

Matlab computer software was used for simulation of the equations that were developed. The results obtained show curves that were similar to those obtained experimentally. The characteristic of the curves obtained show that V_{oc} decreases with the increase in temperature while I_{sc} increases slightly with the increase in temperature.

CHAPTER 1

1.1 INTRODUCTION:

Solar energy has so far been the main source of energy for all living things. To a greater extent, human beings have been relying on fossil fuel over several years. The research that has been conducted so far by BP (2003) and BGR (2003) indicates that due to high rate of population growth, and hence more need for fossil fuel, there is likelihood that crude oil will be depleted in the next 41 years to come, natural gas 61 years and coal will become extinct in 204 years time. This has triggered the researchers to search for an alternative source of energy and have found that there is need to come up with a more reliable source of energy which is cost effective and being human and environmental friendly. They have found out that if solar energy is harvested in a more efficient method, it can replace the fossil fuel. This has called the need for researchers to intensify their research on solar cells which has resulted to the new type of the solar cells called **D**ye **S**ensitized **S**olar **C**ells (**DSSCs**). These are more promising due to the fact that the conventional solid state solar cells which are made of semi-conducting materials such as Germanium (Ge), Silicon (Si) and Cadnium Arsenide (CdAs) are rather expensive particularly when we are dealing with them in their pure form. Manufacturing of these types of solar cells is not cost effective which has discouraged the use of such devices in industrial-scale and solar-electricity production.

DSSC technology has received much attention for development of low cost; though may have low efficiency solar energy conversion. Stangl et al. (1998) found that an efficiency of more than 10% may be reached at considerably lower production costs compared to the conventional p-n junction solar cells. However, not only technological problems (i.e. long term stability) have to be solved, but also the physics of this type of a solar cell is still not understood in details. For instance, though there is a lot of research being carried out on electric model of a DSSC, which relates its structural and chemical properties to its electrical properties there is very little effort being channeled towards studying the effect of temperature on the performance of DSSC. Further improvement highly relies on better understanding of the energy conversion mechanisms and precise modeling for design optimization.

1.2 SUNLIGHT

Sun, just like any other hot body, emits spectral distribution of electromagnetic radiation depending on its temperature. The radiant power per unit area perpendicular to the direction of the sun outside the earth's atmosphere but at the mean earth-sun distance is generally constant. This radiation intensity is essentially referred to as the solar constant or **A**ir **M**ass **Z**ero (AM 0). Understanding of the exact distribution of the energy content in sunlight is very crucial in solar cell work because these cells respond differently to different wavelengths of light.

Green (1992) found that sunlight is attenuated by at least 30% during its passage through the earth's atmosphere due to;

1. Scattering by molecules in the atmosphere.
2. Scattering by aerosols and dust particles.
3. Absorption by particles in the atmosphere.

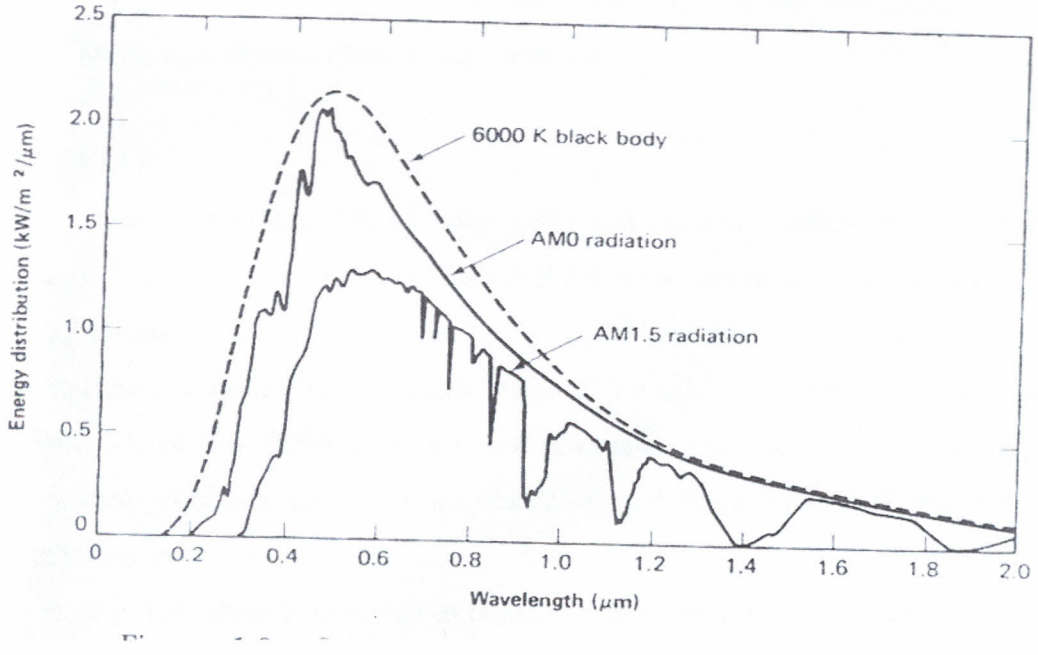

Figure1.1 AM 0 and AM 1.5 shows the spectral distribution of sunlight. Shown are the cases of at 1.5 radiation together with the radiation distribution expected from the sun if it were a black body 600K (Green, M. A. 1992).

A typical spectral distribution of sunlight reaching the earth surface is shown by the lower curve which indicates the absorption bands associated with molecular absorption.

The most important parameter determining the total incident power under clear conditions is the length of the light path through the atmosphere which is shortest when the sun is directly

overhead. The length of any actual path length to this minimum value is known as the **optical air mass**. This means that when the sun is directly overhead, the optical air mass is unity and the radiation is described as air mass one (**AM 1**).

To allow a meaningful comparison between the performances of different solar cells tested at different locations, a terrestrial standard has to be defined and the measurements are referred to this as standard. Although the situation is in a state of flux, the most widely used terrestrial standard is AM 1.5 distributions. According to Green (1992), the total power density content of $100mW/cm^2$ was incorporated as the standard in 1977 which is close to the maximum power received at the earth's surface.

Poor weather causes some regions of the world to receive low level of solar radiation and will also cause a large portion of it to be diffused. Diffused sunlight has a different spectral composition from direct sunlight and it will be richer in the shorter wavelengths.

Photovoltaic systems based on concentrated sunlight can generally only accept rays spanning a limited range of angles. This implies that they usually track the sun to utilize the direct component of sunlight, with the diffuse component wasted.

1.3 SOLAR CELLS

A photovoltaic system consists of solar cells and ancillary components such as power conditioning equipment and support structures. Solar cells utilize the energy from the sun by converting solar radiation directly into electricity. In 2001, International Energy Agency found out that crystalline silicon accounted nearly 74% of the solar cell production. The high costs associated with crystalline silicon solar cell modules are mainly due to the high energy demand for the purification of silicon dioxide from quartz or sand to silicon and to low material yield during the fabrication process.

The future of photovoltaic is believed to belong to thin films solar cells whose cost reduction is achieved by reduced material needed, compared to crystalline solar cells and the possibility of producing large area modules in continuous process. Thin film approaches are usually thought of as those utilizing active semiconductor materials of approximately 10μm or less in thickness.

In the DSSC, a completely different thin film approach is used, based on electrochemistry at the interface between a dye adsorbed onto a porous network of nanometre-sized TiO_2 particles (nanostructure) and an electrolyte. One unique characteristic of this solar cell is the ease with

which it is produced. Low energy demanding processing is attractive from both a cost and an environmental perspective.

Life Cycle Assessment (LCA) is a useful tool for evaluating the environmental impact. In a LCA of a DSSC, it was found that the DSSC system would result in about 20-50g of CO_2 emission per kWh electricity generated compared to 450g CO_2 per kWh for a natural gas power plant. The most significant activity contributing to the environmental impact over the life cycle for the DSSC system is the process in which energy is expended during the solar cell module fabrication.

1.4 DYE SENSITIZED SOLAR CELLS

The dye sensitization concept was invented in order to find a photo-electrochemical solar cell based on a semiconductor, which is stable against photo-corrosion and yet absorb light in the visible region. Many metal oxides fulfill the former requirement; however, most only absorb UV light. A way to extend their spectral response is to adsorb dye molecules absorbing visible light on the semiconductor surface: dye sensitization. By making use of a porous network of nanometer-sized crystals of TiO_2 deposited on a conducting substrate, the TiO_2 surface can become 100 times larger than microscopic area, per micrometer film thickness. The enlarged surface area of TiO_2 leads to increased dye adsorption (by the same factor) resulting in an increased harvesting of sunlight and an increased interface between the dye-sensitized semiconductor and the electrolyte.

1.5 STATEMENT OF PROBLEM

DSSCs are mainly made up of Transparent Conducting Oxide (TCO), thin film of fluorine doped TiO_2 semiconductor as well as an inorganic solvent. TiO_2 is a photo-catalysis used as charge collector and modified for the purpose of modifying spectral range and reduces photo scattering while the electrolyte is used as a medium through which the redox couple can diffuse.

Since the cell has its major components being conductors and the semiconductor, its performance is affected by the change in temperature and therefore it is very important to study the effects of temperature on the overall performance of the DSSCs.

1.6 OBJECTIVES

This project is aimed at developing a theoretical model for studying the optoelectronic properties of DSSCs in relation to temperature change and compare the results with those that have already been obtained experimentally. In this regard, the main factors that have been studied in this project that determine the output of DSSCs are;

1. Open circuit voltage (V_{oc}) and
2. Short circuit current (I_{sc}).

It has been reported by Green (1992) that other solar cell parameters such as fill factor (FF), efficiency (η) and power output heavily rely on V_{oc} which has triggered this research towards it since all Solar cells operate by the same principles.

1.7 JUSTIFICATION AND SIGNIFICANCE OF THE STUDY

From the research that was conducted by both BP (2003) and BGR (2002) revealed that crude oil faces depletion in 41 years time has caused the researchers to embark intensively on alternative sources of energy and particularly the solar cells.

This has in turn raised the concern to come out with a project that is aimed at studying the effects of environmental conditions that do have direct impact upon the output of a solar cell, particularly the temperature. It is in this study that the emphasis is laid on the performance of solar cells at a temperature range of between 25°C (298K) and 55°C (328K), inclusively. This is mainly because most of the solar cell modules are fixed on roof tops where the temperature is within the range of this study.

From the outcome of this project, it is anticipated that the designers of the solar cell modules will improve on the structures. Furthermore, those who fix them on roof tops will also be considering the material, colour of the underlying surface and whether or not it should be in contact with the roof top with the aim of maximizing the incident photon to current-conversion efficiency (IPCE).

CHAPTER 2

PHYSICS OF SOLAR CELLS

2.1 INTRODUCTION

Since power can be delivered to an external circuit by an illuminated p-n junction, it is possible to covert solar energy into electrical energy. In this case, Streetman (2004) found out that, output voltage is restricted to values less than contact potential, which is in turn less than band gap voltage Eg/q. The current generated depends on the illuminated area. This means that to utilize a maximum amount of available optical energy, it is necessary to design a solar cell with a large area junction (active area) located near the surface of the device.

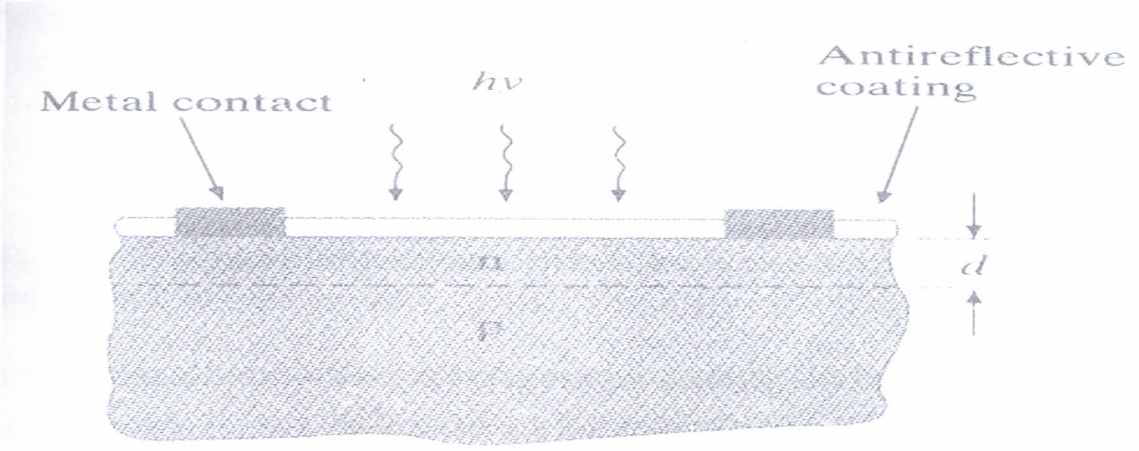

Figure 2.1 Configuration of a solar cell showing an enlarged view of the planer junction (Streetman and Banerjee, 2004).

The junction depth, d, must be less than hole diffusion length L_p in the n material to allow holes generated near the surface to diffuse to the junction before they recombine; similarly, the thickness of p region must be such that the electron generated in this region can diffuse to the junction before recombination takes place. This shows that there should be a proper match between the electron diffusion length L_n, the thickness of the p region, and the mean optical penetration depth $1/\alpha$, (see equation 2.10 below), where α is optical absorption coefficient.

To obtain higher photo-voltage, it is desirable to have a large contact voltage V_o and therefore heavy doping is necessary; on the other hand, long lifetimes are desirable and these are reduced by heavy doping.

2.2 CURRENT- VOLTAGE IN AN ILLUMINATED JUNCTION.

Current that is generated across a junction of a conventional solar cell is due to drift of minority carriers that are generated within the depletion region, W, and are separated by the junction field as shown below:

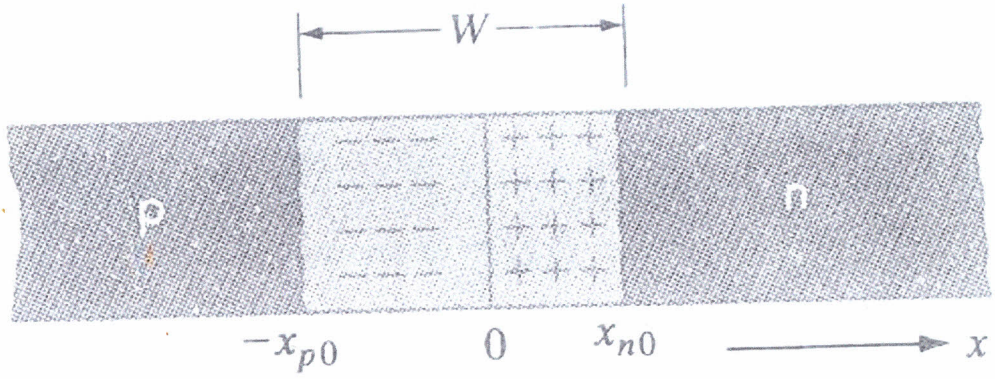

Figure 2.2 Space charge and electric field distribution within the transition region of a p-n junction (Streetman and Banerjee, 2004).

Electrons are collected in the n-side while holes in the p-side. There are also thermally generated minority charge carriers within a diffusion length (L) of either side of the junction which diffuse into the depletion region and are swept to the other side by the electric field. If the junction is uniformly illuminated by incident photons whose energy $h\nu > E_g$, there is an added generation rate g_{op} of electron hole pairs (EHPs/cm^3–s) which participate in this current.

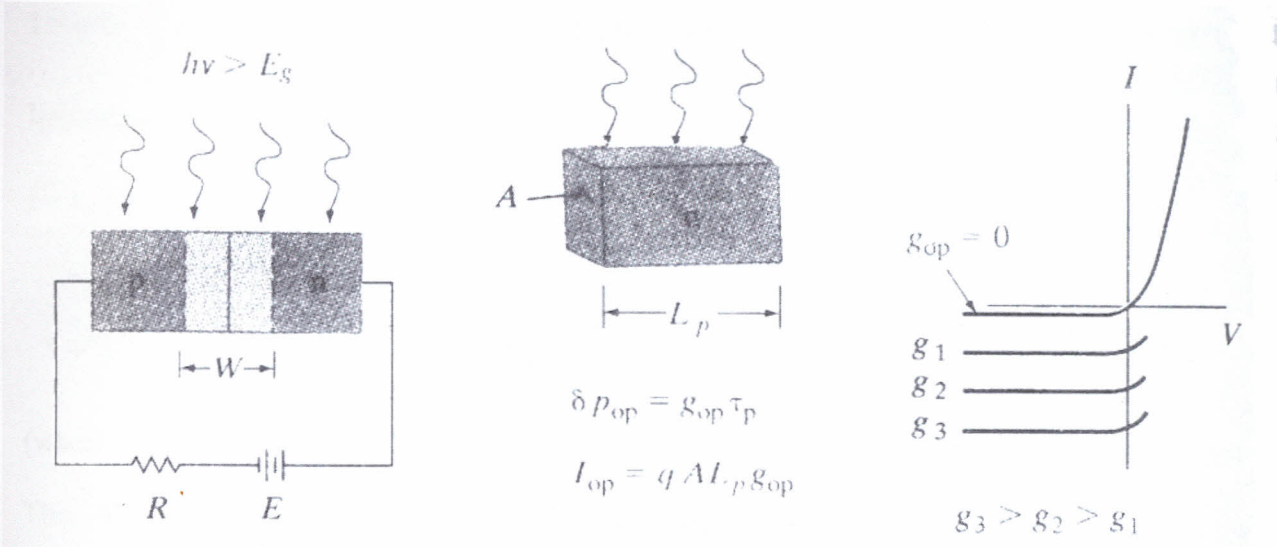

Figure2.3 (a) (b) (c)

Optical generation of carriers in a p-n junction: (a) absorption of light by the device; (b) current I_{op} resulting from EHP generation within a diffusion length of the junction on the n side; (c) I-V characteristics of an illuminated junction (Streetman and Banerjee, 2004).

The I_{op} is the optically generated current which resulted from EHP generation within a diffusion length L_p of the junction on n-side.

The number of holes created per second with the diffusion length of the transition region on the n side is AL_pg_{op}, where A is the cross-section area.. Likewise, AL_ng_{op} electrons are generated per second within L_n of x_{po} while AWg_{op} carriers are generated within W.

The total current as a result of collection of these optically generated carriers by the junction is

$$I_{op} = qAg_{op}(L_p + L_n + W) \quad \text{.....2.1}$$

if

$$qA(\frac{D_p p_n}{L_P} + \frac{D_n n_p}{L_n}) = I_0 \quad \text{.....2.2}$$

denotes thermally generated current I_{th}, where D_p, p_n, L_p, D_n, n_p and L_n are hole diffusion constant, hole concentration in n-side, hole diffusion length, electron diffusion constant, electron concentration in p-side and electron diffusion length, respectively, we can add the optical generation of equation (2.1) to find the total reverse current when the diode is illuminated. Since the current flows from n to p, the diode equation

$$I = qA\left(\frac{D_p p_n}{L_p} + \frac{D_n n_p}{L_n}\right)\left(e^{\frac{qV}{KT}} - 1\right) = I_o\left(e^{\frac{qV}{KT}} - 1\right) \quad \text{.....2.3}$$

becomes

$$I = I_{th}\left(e^{\frac{qV}{KT}} - 1\right) - I_{op}$$

$$= qA\left(\frac{L_p p_n}{\tau_p} + \frac{L_n n_p}{\tau_n}\right)\left(e^{\frac{qV}{KT}} - 1\right) - qAg_{op}(L_p + L_n + W) \quad \text{.....2.4}$$

(where $L_p = \sqrt{D_p \tau_p}$ and $L_n = \sqrt{D_n \tau_n}$)

This implies that the I-V curve is lowered by an amount proportional to the generation rate as shown in figure 2.3c.

Equation (2.4) above has two components, namely, the part due to optical generation and the current described by the diode equation. When the diode is short circuited, the first term on the right hand side of equation (2.4) disappears because V= 0 and the short circuit current (I_{op}) flows from n to p which cuts the I-V curve at a negative value as shown in figure 2.3c above. It is worth noting that I_{op} is proportional to g_{op}.

When there is an open circuit I = 0 and V = V_{oc} equation (2.4) then reduces to

$$V_{oc} = \frac{KT}{q}\ln\left(\frac{I_{op}}{I_{th}} + 1\right) = \frac{KT}{q}\ln\left[\frac{L_p + L_n + W}{(L_p/\tau_p)p_n + (L_n/\tau_n)n_p} \times g_{op} + 1\right] \quad \text{.....2.5}$$

For a case of asymmetrical junction, $p_n = n_p$ and $\tau_p = \tau_n$ equation (2.5) after neglecting generation within W and +1 to reduce to

$$V_{oc} = \frac{KT}{q}\ln\frac{g_{op}}{g_{th}} \quad \text{.....2.6}$$

where $g_{op} >> g_{th}$ and $g_{th} = \frac{p_n}{\tau_n}$ is the thermal generation rate which represents the equilibrium thermal generation- recombination rate.

As the minority carrier concentration is increased by optical generation of EHPs, the lifetime τ_n becomes shorter, and $\frac{p_n}{\tau_n}$ becomes large (p_n is fixed for a given N_d and T). This implies that, according to Streetman (2004), Voc can not increase indefinitely with increased generation rate but has the limit at equilibrium contact potential Vo as shown below:

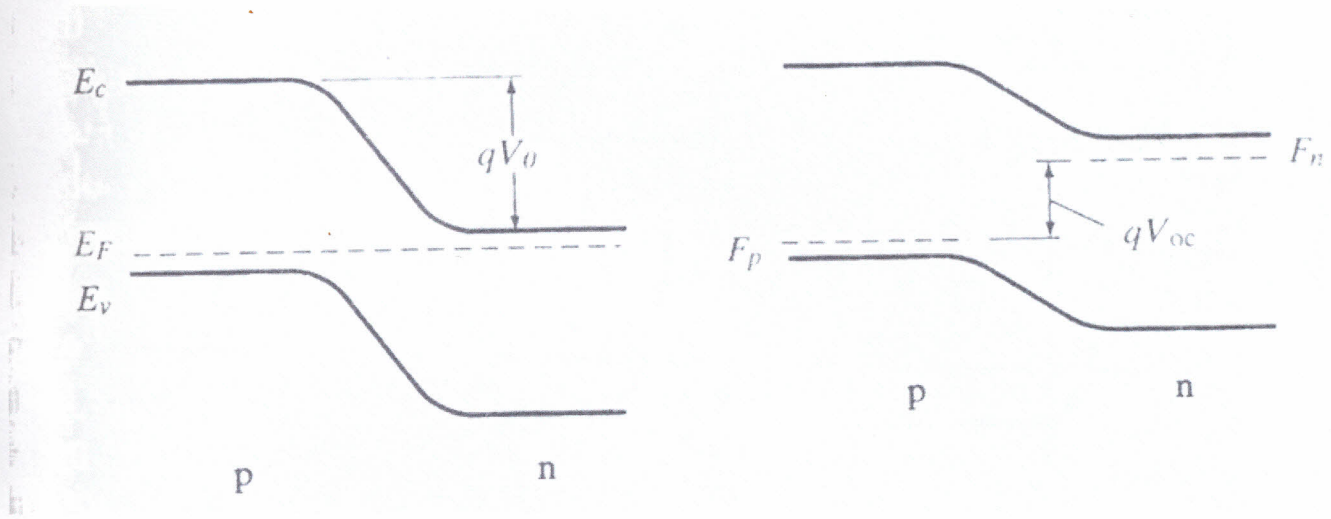

(a) (b)

Figure 2.4 Effect of illumination on the open circuit voltage of a junction: (a) junction at equilibrium; (b) appearance of a voltage V_{oc} with illumination (Streetman and Banerjee, 2004).

This illumination is true since contact potential is the maximum forward bias that appear across a junction. The appearance of a forward voltage across an illuminated junction is known as the photovoltaic effect.

Depending on the intended application, Streetman (2004) observed that, photodiode can be operated on the 3rd or 4th quadrant of its I-V characteristic as shown in figure 2.5 below.

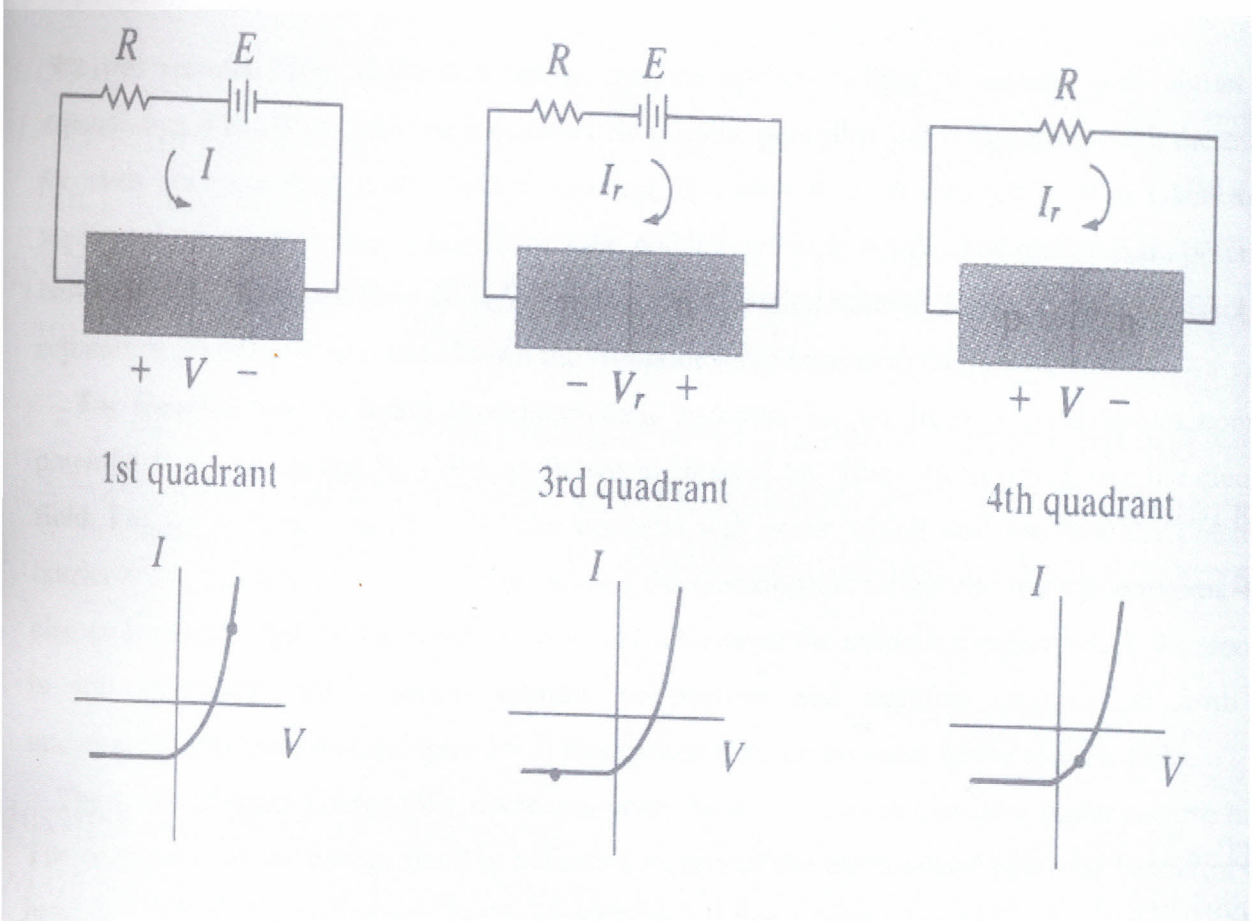

Figure 2.5 (a) (b) (c)

Operation of an illumination junction in the various quadrants of its I-V characteristics in; (a) and (b) power is delivered to the device by the external circuit while in (c) the device delivers power to the load (Streetman and Banerjee).

In (a) and (b) power is delivered to the device by the external circuit as long as both current (I) and voltage (V) have the same sign but in (c) the device delivers power to the load where I is negative and V is positive. The current in (c) flows from the negative side of V to the positive side, as in a battery.

This implies that the fourth quadrant is used when the power is being extracted from the device while in photo-detectors, we reverse bias the junction and operate it in the 3rd quadrant.

2.3 QUALITITIVE DESCRIPTION OF CURRENT FLOW AT A JUNCTION.

We first assume, from figure 2.6 below, that the applied voltage V appears only across the transition region (W) of the junction rather than in the neutral n and p regions though there will be some potential drop in the neutral material, if a current flows through it. V is taken to be positive if the external bias is positive on the p side relative to n side. The electrostatic potential barrier and thus, electric field changes as a result of applied voltage. This will in turn affect the separation of energy bands and also all the components of current at the junction.

The forward bias V_f lower the electrostatic potential barrier from its equilibrium contact potential V_0 by the factor $V_0 - V_f$ as shown in figure 2.6b. This will in turn lower the electric field. For the reverse bias ($V= -V_r$) the opposite will occur which will increase the potential barrier at the junction ($V+V_r$) while increasing the electric field within the transition region. The change in electric field at the junction calls for a change in the transition region width W, since it is still necessary that a proper number of positive and negative charges (in form of uncompensated donor and acceptor ions) be exposed for a given value of the electric field.

The width of space charge (W), decreases under forward bias and increases under reverse bias. The separation of the energy band is a direct function of the electrostatic potential barrier at the junction. The shifting of energy bands under bias implies a separation of Fermi-levels on either side of the junction.

Under forward bias, the Fermi level on the n-side E_{Fn} is above E_{Fp} by the energy qV_f ; for reverse bias, E_{Fp} is qV_r joules higher than E_{Fn} . The Fermi levels in the two neutral regions are separated by an energy (eV) numerically equal to the applied voltage (V).

The diffusion current is composed of electrons which are the majority charge carrier in n-side surmounting the potential energy barrier to diffuse to the p-side, and likewise the holes from p-side to n-side.

The electron drift current as a result of minority carriers depends on how many electrons are swept down the barriers per second just like the drift of minority holes from n to p side of the junction and both electrons and holes drift current are independent of the applied voltage.

The supply of the minority carriers entirely on the either side of the junction required to participate in the drift component of current is generated by thermal excitation of electron hole pairs (EHPs). The resulting current due to drift of generated carriers across the junction is

commonly called the generation current since its magnitude depends the rate of generation of EHPs.

The total current crossing the junction is composed of the sum of the diffusion and drift components. The diffusion current due to electrons and holes move from p to n (although the particle flow directions are opposite to each other) and the drift currents are from n to p.

Figure 2.6 below shows the effect of a bias at a p-n junction; transition region width and electric field, electrostatic potential, energy band diagram, and particle flow and current directions within W for;

(a) Equilibrium.

(b) Forward bias and

(c) Reverse bias.

The numerals represent;

(1) Hole diffusion.

(2) Hole drift.

(3) Electron diffusion.

(4) Electron drift.

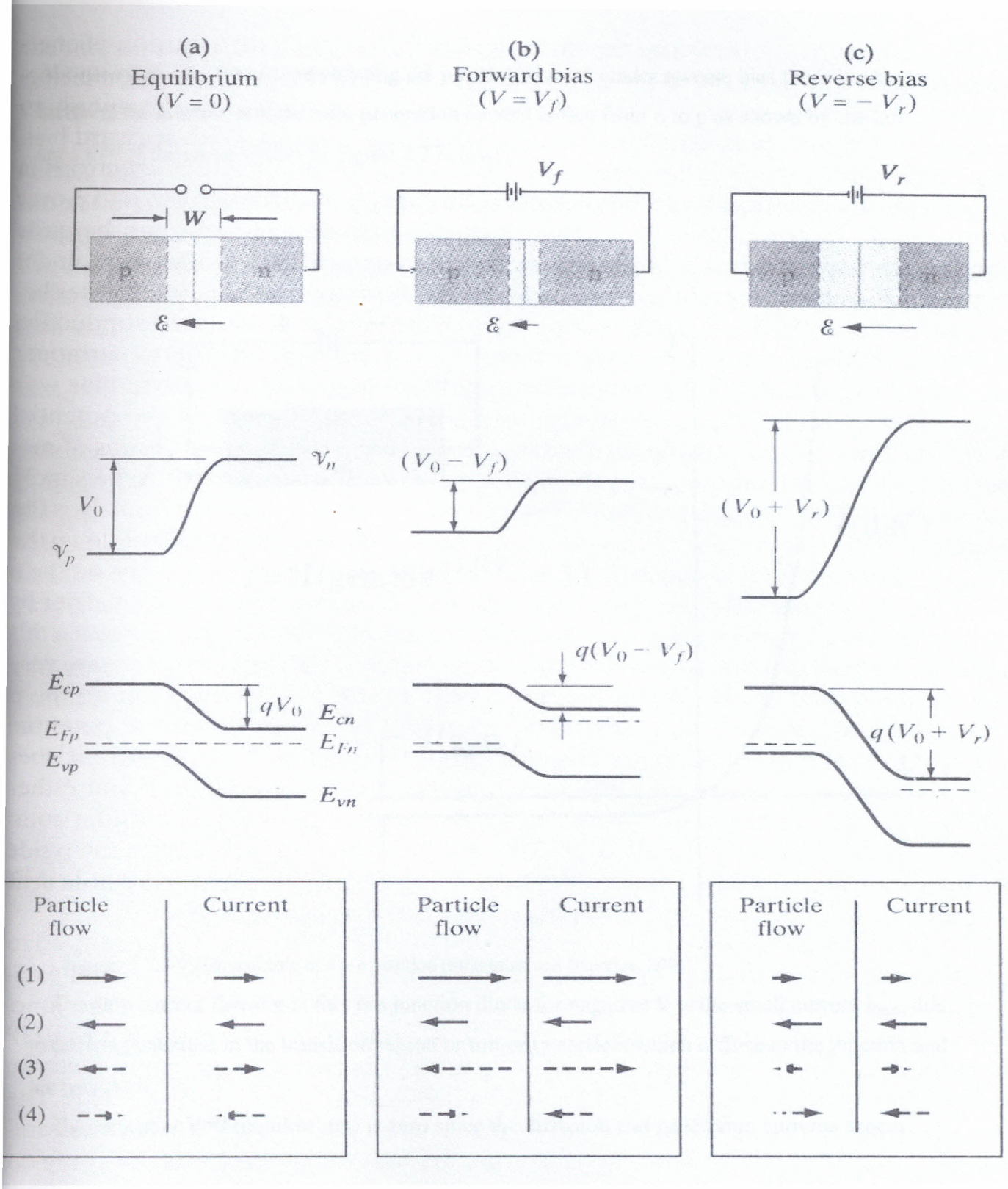

Figure 2.6 Effect of a bias at a p-n junction; transition region width and electric field, electrostatic potential, energy band diagram , particle flow and current directions within W for (a) equilibrium, (b) forward bias, and (c) reverse bias (Streetman and Banerjee, 2004).

At equilibrium, the net current crossing the junction is zero. Under reverse bias there is a large barrier at the junction and the only generation current is that from n to p as shown by the left hand side of the curve shown by figure 2.7 below;

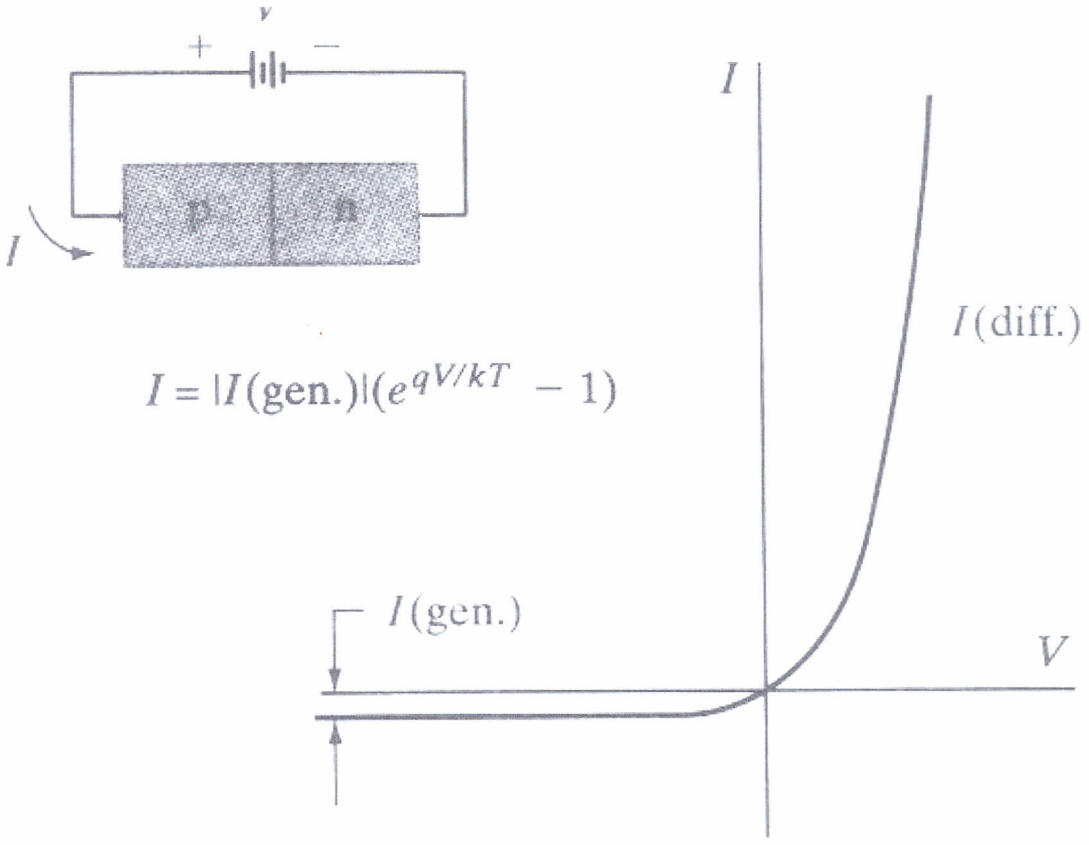

Figure 2.7 I-V characteristic of a p-n junction (Streetman and Banerjee, 2004).

The only current flowing in this p-n junction diode for negative V is the small current $I_{(gen)}$ due to carriers generated in the transition region or minority carriers which diffuse to the junction and are collected.

The current at V=0 (equilibrium) is zero since the diffusion and generation currents cancel.

$$I = I_{(diff)} - \left|I_{(gen)}\right| = 0 \quad \text{.....2.7}$$

It is worth noting that an applied forward bias voltage V $=V_f$ increases the probability that a carrier can diffuse across junction; by the factor $\exp(\frac{qV_f}{kT})$. Thus the diffusion current under forward bias is given by its equilibrium value multiplied by $\exp(\frac{qV}{kT})$; similarly, for reverse bias the diffusion current is the equilibrium value reduced by the same factor, with V= - V_r. Since the equilibrium diffusion current is equal in magnitude to $|I_{(gen)}|$, the diffusion current with applied bias is simply $|I_{(gen)}| \exp(\frac{qV}{kT})$. The total current I is given by the diffusion current less absolute value of the generation current, which can be referred to as I_o;

$$I = I_o [\exp^{(\frac{qV}{kT})} - 1] \quad \text{.....2.8}$$

and if

$$I_o = qA(\frac{D_p p_n}{L_p} + \frac{D_n n_p}{L_n}) \quad \text{.....2.9}$$

then, the above equation becomes the diode equation.

2.4 EXCESS CHARGE CARRIERS IN SEMICONDUCTORS

Most semiconductor devices operate by the creation of the charge carriers in excess of the thermal equilibrium values. Incase of the solar cells, these excess charge carriers are created by optical excitation. It is worth noting that photons with energies greater than the band gap energy $h\upsilon > E_g$ are absorbed while those with energies less than the band gap are transmitted. Optical absorption causes an electron to be excited from valence band which contains many electrons to the conduction band which has many empty states. The EHPs created by this absorption process are excess carriers and are free to contribute to the conductivity of the material. In a pure semiconductor, there is negligible absorption of photons with $h\upsilon < E_g$ and this explains why some materials are transparent in certain wavelength ranges.

If the band gap is about 2eV wide, only long wavelengths (infrared) and the red part of the visible spectrum are transmitted; on the other hand, a band gap of about 3 eV allows infrared and the entire visible spectrum to be transmitted.

The ratio of transmitted incident light intensity depends on photon wavelength and the thickness of the sample. To get this dependence, we can let the intensity of incident photon beam be denoted by $\mathbf{I}_0$ (photons / cm^2-s) which is incident upon a sample of thickness d. In this case, we assume that we are dealing with a monochromatic radiation of wavelength λ. As the beam passes through the sample, its intensity at distance x from the surface can be calculated by considering the probability of absorption within an increment dx. The probability of absorption of photon which has survived to point x within the material is constant. This implies that the degradation of the intensity $\frac{-d}{dT}\mathbf{I}(x)$ is proportional to the intensity remaining at x

$$\frac{-d}{dT}\mathbf{I}(x) = \alpha \mathbf{I}(x) \quad \text{.....2.10}$$

solving

$$\mathbf{I}(x) = \mathbf{I}_0 e^{-\alpha x} \quad \text{.....2.11}$$

where α is the absorption coefficient.

2.5 SOLAR CELL DESIGN

The DSSC consists of a working electrode, a counter electrode and an electrolyte. It can be made from a variety of materials. The simplest method is whereby a 5μm to10μm thick nanostructured TiO_2 film is deposited onto a transparent conducting substrate. The dye sensitized TiO_2 forms the working electrode. A platinized conducting substrate constitutes the counter electrode of the solar cell.

The dye N719 is adsorbed on the surface of the nanostructured TiO_2 film by soaking the film in an ethanoic solution of N719. The bonding between the dye and the TiO_2 should give high stability, dense packing and efficient charge injection. The dye absorbs light between 300nm to 800 nm.

An electrolyte is attracted into inter-electrode space (≈50% porosity) of the nanostructured dye sensitized film by the capillary force. The electrolyte should have high conductivity and be able to penetrate the nanostructured system. These requirements are best matched by a liquid electrolyte. The redox system iodide/triiodide dissolved in an organic solvent is the basis of the electrolyte. Organic solvents are used instead of the water based ones, since the dye is unstable in water. The mixing of salt of iodine and a salt of iodide forms the iodide/triiodide.

CHAPTER 3

3.1 STRUCTURE OF A DYE SENSITIZED SOLAR CELL

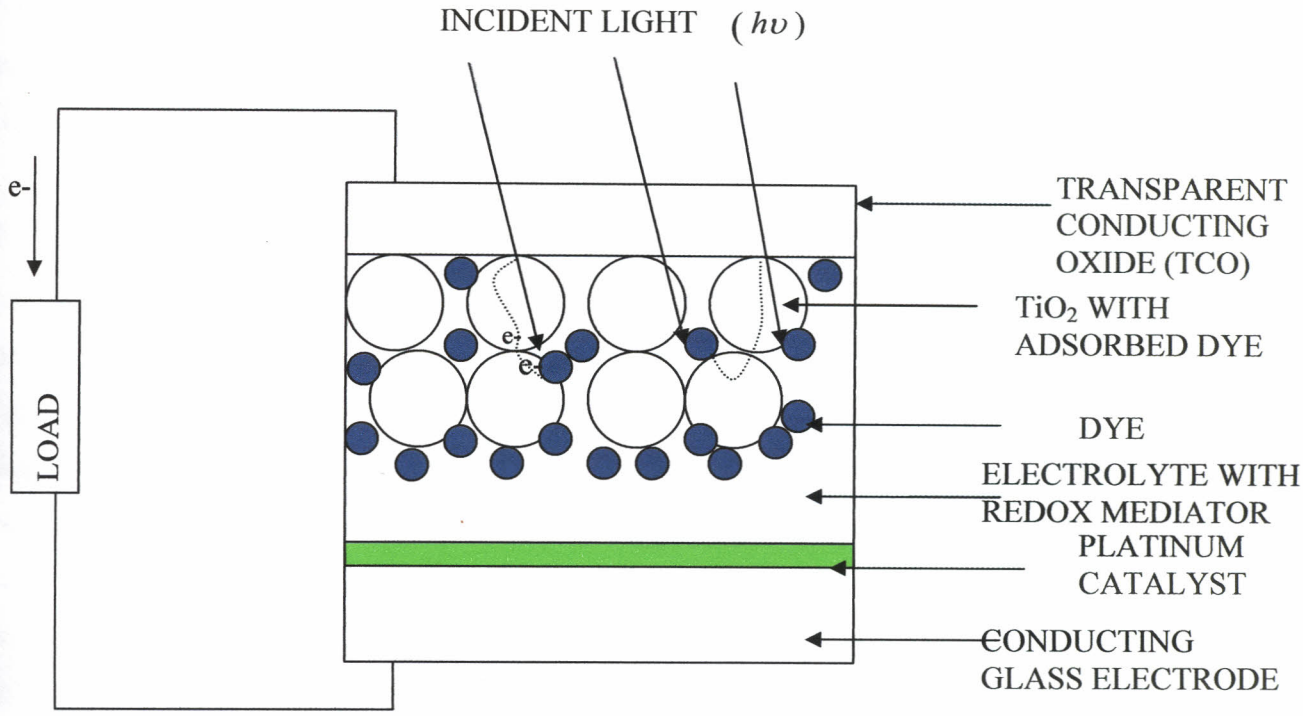

Figure 3.1 schematic diagram of a Dye Sensitized Solar Cell (DSSC).

DSSCs comprises of a nanocrystalline TiO_2 electrode modified with a dye fabricated on a transparent conducting oxide (TCO), a platinum (Pt) counter electrode and an electrolyte solution with a dissolved iodide ion/triiodide ion redox couple between the electrodes.

3.1.1 TRANPARENT CONDUCTING OXIDE (TCO)

These are doped oxide based thin film made of transparent conductors such as Tin (Sn) which has shown an excellent optical and electrical properties. Doping is accomplished by replacing some Oxygen with Fluorine to form Fluorine doped Tin Oxide ($F:SnO_2$) substrates. Granqvist (2007) found that a specific advantage of the TCOs, compared to their noble metal- based counterparts, is the chemical and mechanical stability, which allows their use on glass surfaces exposed to the ambience; the oxide film are sometimes referred to as 'hard coats'. The basic reason why transparent conductors are of concern is that they can show transparency in a limited and well defined range, normally encompassing visible light in the

$0.4\mu m < \lambda < 0.7\mu m$ wavelength interval. In the infra-red (IR) their metallic properties leads to reflectance and at sufficiently short wavelengths, in the ultraviolet (UV) they become absorbing due to excitation across an energy gap.

The DSSC has two TCO materials; one on the upper part of the cell whose lower side is sputtered with TiO_2 nona-particles while the other has its upper part sputtered with platinum acting as a catalyst for the redox reaction as shown in figure 3.1.

3.1.2 TITANIUM DIOXIDE (TiO_2)

This is the oxide of the metal titanium used as the white pigment in paints. A water based solution of commercial nanocrystalline titanium dioxide (TiO_2) powder is used to deposit a highly porous semiconductor electron acceptor. This acceptor couples the light driven processes occurring at an organic dye to the microscopic world and an external electrical circuit.

In the present era of ecological and environmental consciousness, TiO_2 is preferred for it is inert, non-toxic compounds. It is cheap and readily available material. Kalyanasundaram and Gratzel (1998) reported that TiO_2 exists in three common crystalline polymorphs namely Rutile, Anatase and Brookite. Rutile is most widely used because it is thermodynamically most stable and its transformation to anatase occur between 700-1000^{0}C depending on its purity content and crystallite size. TiO_2 is a wide band gap semiconductor where the band gap energies of rutile is 3.0 eV while that of anatase is 3.2 eV (at 0K). It is widely used for light energy conversion. The advantage of utilizing nanocrystalline TiO_2 films is that TiO_2 is a very stable material having a very high refractive index and has a very good light transmittance optical properties.

Since the energy gap of anatase at 0K is about 3.2 eV, from the energy equation

$$E = \frac{hc}{\lambda} \quad \text{.....3.1}$$

where E is the energy equivalent of TiO_2 band gap, h is Planck's constant, c is the velocity of electromagnetic radiation while λ is the corresponding wavelength and after rearranging equation 3.1, we have

$$\lambda = \frac{hc}{E} \quad \text{.....3.2}$$

and after substituting for h, c and E with their appropriate values we get that

$$\lambda \approx 387.5\,\text{nm}. \quad \ldots\ldots 3.3$$

This indicates that TiO_2 absorbs light in UV region and transmits in the visible and the near infra-red ranges.

3.1.3 THE DYE

The active semiconductor (photoelectrode) that is used in DSSCs is a wide band gap oxide semiconductor like TiO_2, SnO_2, ZnO_2 etc. The disadvantage due to their large band gap is overcome by a proper choice of a dye to sensitize the semiconductor.

When light is incident onto DSSC, it passes through the outer glass cover (not shown in the diagram), then through TCO, then through TiO_2 nanocrystals and is eventually absorbed by the dye particles which are adsorbed on TiO_2 nanoparticles.

TiO_2 is coated with a monolayer of a suitable charge transfer dye, which acts as sensitizer. The dye absorbs the solar energy whereas the TiO_2 is responsible for the charge-carrier transport. Since light absorption occur mainly at the photosensitive dye, it is therefore necessary to increase the Incident (monochromatic) Photon-to-electron Conversion Efficiency (IPCE) of photosensitive electrodes with dye. Light harvest efficiency (LHE) depends heavily on;

1. The properties of the dye, such as extinction coefficient, absorbance and dye uptake on TiO_2 electrode.
2. Optical path length within the electrodes.

Many dyes, including organic dyes and transition metal complexes, have been employed in DSSCs. The advantage of organic dyes is their high molar extinction coefficient.

Ruthenium (11)-based charge-transfer polypyridyl complexes show the highest energy conversion efficiency. This is due to; intense Charge-Transfer (CT) as a result of light absorption in the whole visible range, moderately intense emission with fairly long lifetime in fluid solutions at ambient temperature, high quantum yield for the formation of the lowest CT excited state, the redox reactivity and ease of tunability of redox properties.

If the TiO_2 particles are too small, the pores are not large enough for the dye and the electrolyte to enter. If the particles are too large, there is not enough internal surface area for the

dye adsorption. Photo conductivity of the TiO_2 electrode depends on the particle size. Dye that can be utilized should have a chemical group which can attach and adsorb on TiO_2 and must have the following properties;

1. It should absorb all light below a threshold wavelength of about 920 nm.
2. It must carry attachment groups such as carboxylate or phosphonate to firmly graft it to the semiconductor oxide surface.
3. Upon excitation, it must inject electrons into the solid with a quantum yield of unity.
4. Its energy level at excited state should be slightly above the lower bound of the conduction band of the oxide to minimize energetic losses during the electron transfer reaction.
5. Its redox potential should be positive so that it can be regenerated through electron donation from the redox electrolyte or the hole conductor.
6. It should be stable to sustain about 10^8 turnover cycles corresponding to about 20 years of exposure to natural light.

3.1.4 ELECTROLYTE

The current in liquid electrolytes is carried by ions which are formed by the dissociation of salts in polar solvents. In contrast to the situation with semiconductors, where there are also two types of charge carriers (electrons and holes) but one type usually dominates because of doping, both types of carriers (positively and negatively charged ions) are always in equal concentrations in electrolyte. The electrolyte in the DSSCs consists of a redox couples dissolved in a solvent. Redox couple are characterized by molecules or ions (in solution) which can be in a reduced state (Red) or an oxidized state (Ox) in electron transfer reaction. If this species accepts an electron, it changes from an oxidized to a reduced state. Conversely, giving up an electron or accepting a hole oxidizes it. Such species are known as redox couples. The redox couple used for DSSCs is the $I^-/\ I_3^-$ system whereby the iodide (I^-) prevents the recombination of the electron by the oxidized dye and the triiodide (I_3^-) uptakes the electrons at the counter electrode. The electrolyte in these cells serves only to transfer charges between the metal and the semiconductor.

Electrolyte in a DSSC is responsible for the regeneration of the sensitizer. It limits the speed at which the dye molecules can regain their electron and become available for photo excitation. It consists of a solvent with dissolved redox couples. Comparable to conduction and valence bands in semiconductors, G'omezle'on (2001) found that, electrolyte has respectively empty and occupied energy levels. The distribution of energy levels associated with redox couple will define the tendency to donate or accept electrons when redox molecules approach the solid electrode. Due to fluctuation in the solvation shell surrounding the redox molecules, the energy state of redox couples are distributed over a certain range. This implies that by assuming a harmonic oscillation of the solvation shell, the density of occupied states (D_{red}) and those of the empty states (D_{ox}) can be distributed by Gaussian types of functions given below;

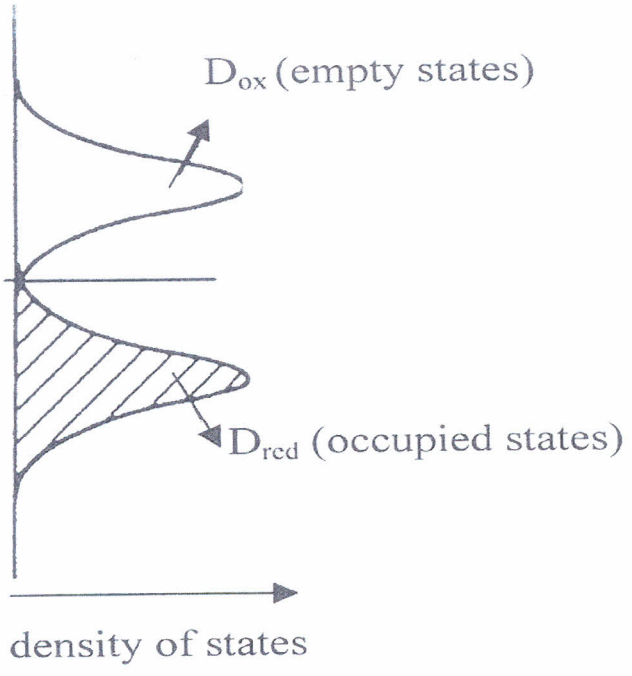

Figure 3.2 Distribution function of the redox system (G'omezle'on 2001).

The energy position of the level of the dissolved oxidized and reduced forms is in the maximum of the Gaussian function and the intersection of the distribution represents the entire solution redox potential which is a result of the redox couple $_{red/ox}$. Since this point represents the stage

where the probability of a level being occupied by an electron is $\frac{1}{2}$, $qV_{red/ox}$ can be considered as the Fermi level in the liquid phase.

3.2 NANO-CRYSTALLINE DSSC OPERATION PRINCIPLE.

The novel nanocrystalline solar cells developed, work on a different principle, as compared to convectional solid state solar cells because the process of light absorption and charge separation are themselves different. Light absorption is performed by a single layer of dye that is chemically attached to the rough surface of a layer of interconnected TiO_2 particles painted on a conductive transparent glass. The minute particles of TiO_2 are single crystals that are each between 10×10^{-9}m and 50×10^{-9} m in size and, because of this, is called nanocrystalline. Due to the very small TiO_2 particle size together with the very strong screening effect of electrolyte, there is no significant macroscopic electric field in most of the porous TiO_2 thin film. Therefore, both electrons and mediators are transported mainly by diffusion.

After having been excited by the light, the coloured dye, usually a ruthenium-based organic compound, is able to transfer an electron to the semi-conducting TiO_2 layer via a process called electron injection or sensitization. The porous TiO_2 layer facilitates the transport of electron to the conductive layer on the glass where it is collected. The oxidized dye molecules are regenerated by the redox mediators, such as Iodide/Triiodide couple I^-/I_3^-, such that the oxidized mediator, I_3^-, brings the positive charge from the dye to opposite side of the cell which is called Counter Electrode. After traveling through the electrical load the electron collected at TCO side of the cell reacts at the counter electrode and the mediator is returned to its original reduced form, I^-. Since the dye layer is so thin, almost all of the excited electrons produced from light absorption can be injected into the TiO_2 and this sensitizes it to the wide range of wavelengths, or colours, of light absorbed by the dye.

The electron photo injection from excited dye to TiO_2 conduction band increases the electron density in the porous electrode thin film, shifting the quasi-Fermi level (E_F) of TiO_2 and TCO closer to the conduction edge (E_C).

In conclusion, it is worth noting that nanocrystalline DSSC is a photo-electrochemical cell that resembles natural photosynthesis in two aspects:

1. It uses the organic dye like chlorophyll to absorb light and produce a flow of electrons.
2. It uses multiple layers to enhance both light absorption and electron efficiency.

3.3 ENERGY DIAGRAM AND THE ASSOCIATED INTER-FACIAL ELECTRON –TRANSFER AT THE DYE SENSITIZED NANOCRYSTALLINE TiO_2.

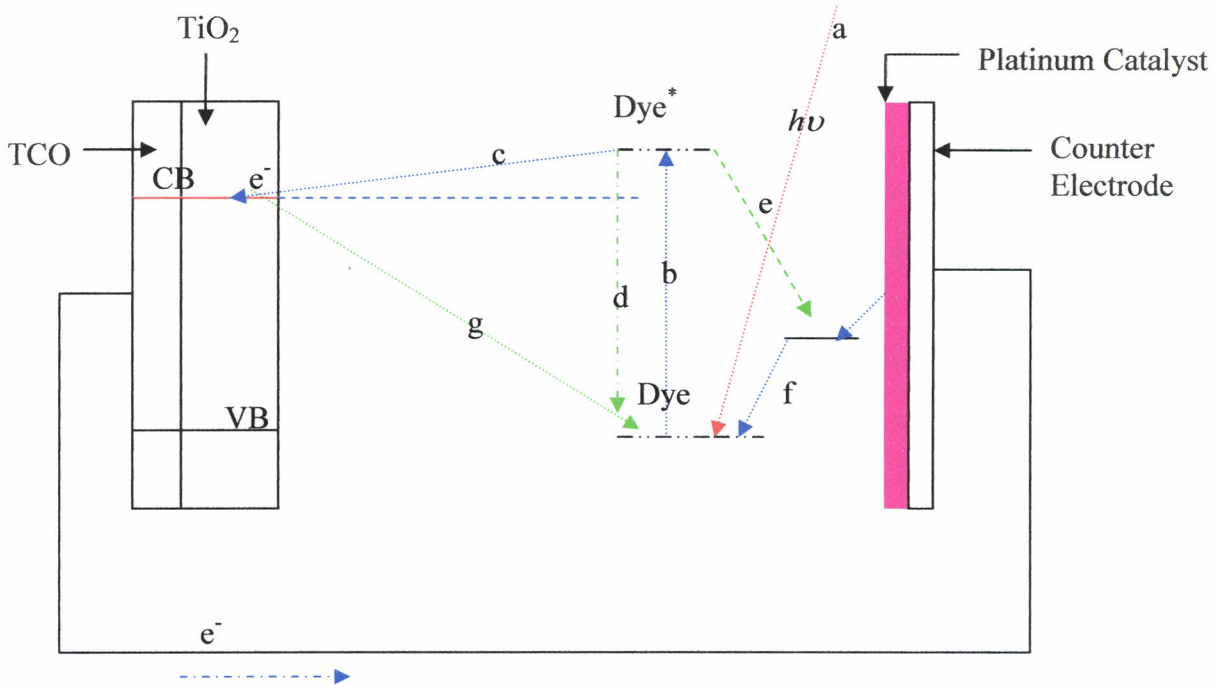

Figure 3.3 Energy level diagram showing charge production and recombination processes.

The voltage produced by the nanocrystalline solar cell is the difference in the energy levels between the TiO_2 conduction band and the mediator, and depends on the mediator and solvent used as well as the condition of the TiO_2 and the intensity of illumination.

The following are the major processes through which the charges are produced as well as the charge recombination processes (which lowers the efficiencies of DSSC):

(a) Light shines on the dye.

(b) The dye gets excited after absorption of photon of energy hυ.

Dye + Light → Dye*

(c) Electrons are injected from the excited dye* molecules and diffuse into the conduction band (CB) of TiO_2.

$$Dye^* + TiO_2 \rightarrow e^- (TiO_2) + \text{oxidized dye.}$$

(d) Thermally decay of excited dye to the ground state.

(e) Quenching of excited dye by electron transfer to oxidized species in the electrolyte solution.

(f) The oxidized dye cation is reduced by redox species present in the electrolyte (regeneration).

$$\text{Oxidized Dye} + \frac{3}{2} I^- \rightarrow \text{Dye} + \frac{1}{2} I_3^-$$

(g) Electron transfer from the photo injected electrons in the conduction band of the semi-conductor to the dye cation (recombination) competes with the reduction of the dye by species in electrolyte solution.

(h) Other electron-transfer processes which produces cathodic currents that opposes the photocurrent includes the reaction between electrons in the membrane and oxidized redox in the electrolyte (direct reduction) and the reaction between electron in the conduction substrate and the electrolyte (leakage current).

Finally, the oxidized redox mediators are regenerated by receiving electrons from the counter electrode for a complete cycle of DSSC energy conversion.

$$\frac{1}{2} I_3^- + e^- \text{(counter electrode)} \rightarrow \frac{3}{2} I^-$$

CHAPTER 4

4.1 PHOTO-VOLTAIC DEVICE CHARACTERISTICS.

The electrical properties of conventional p-n junction solar cells can be analyzed by using an equivalent circuit consisting of a current generator, a photosensitive diode, a shunt and a series resistor as shown in figure 4.1 below;

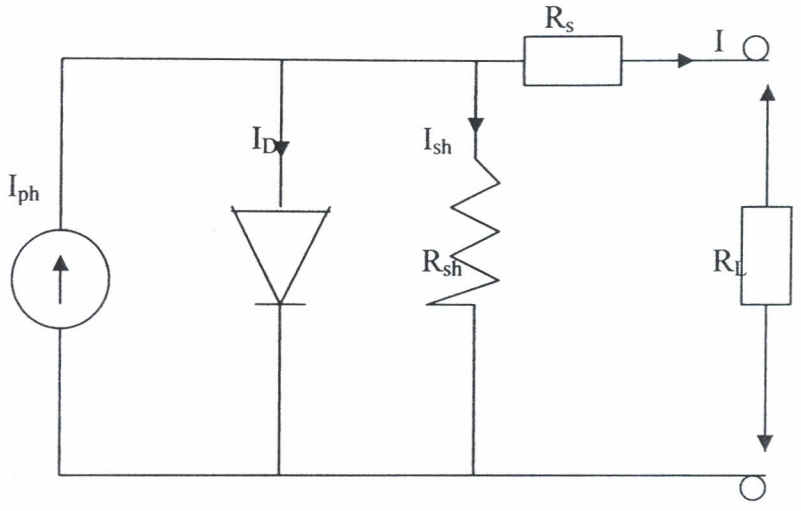

Figure 4.1 Simple equivalent circuit model for conventional p-n junction solar cells. This model consists of a constant current source (I_{ph}), a diode, series resistance (R_s) and shunt resistance (R_{sh}).

I-V characteristics of solar cells are described based on the Schottky equation for thermionic emission which is expressed by Wanzeller et al. (2004) as

$$I = I_{ph} - I_D - I_{sh} \quad \text{.....4.1}$$

or

$$I = I_{ph} - I_o\{\exp[\frac{q(V + IR_s)}{nkT}] - 1\} - \frac{V + IR_s}{R_{sh}} \quad \text{.....4.2}$$

This can be verified by realizing that a solar cell is simply a diode in which its current from I-V curve has been lowered from zero to I_{sc} of the solar cell. This shift is caused by the fact that a photovoltaic cell is an active current producing device.

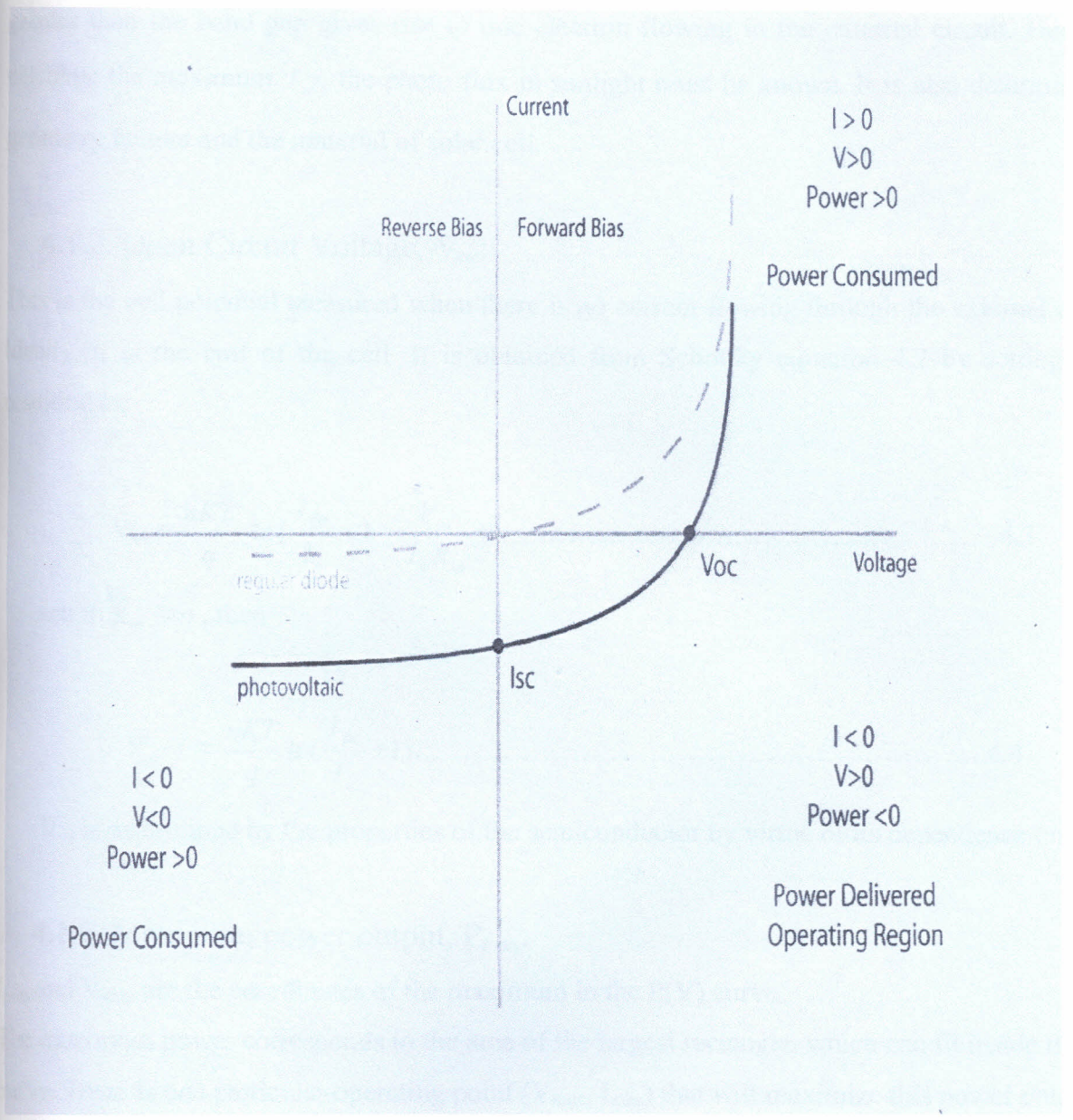

Figure 4.2 Photovoltaic relative to a diode

In order to analyze photo current-voltage curves, one should determine the following parameters:

4.1.1. Short circuit current, I_{sc} :

It is as a result of excitation of excess carriers by solar radiation. It is measured at an applied potential of zero volts as shown in figure 4.2 above.

Ideally, this is equal to light generated current. It is a function of illumination intensity, if the spectral distribution of radiation is not varied, because each photon incident on the cell of energy greater than the band gap gives rise to one electron flowing in the external circuit. Hence, to calculate the maximum I_{sc}, the photo flux in sunlight must be known. It is also determined by geometry factors and the material of solar cell.

4.1.2. Open Circuit Voltage, V_{oc}:

This is the cell potential measured when there is no current flowing through the external circuit. Ideally, it is the emf of the cell. It is obtained from Schottky equation 4.2 by setting $I_0 = 0$ resulting to;

$$V_{oc} = \frac{nKT}{q} \ln\{\frac{I_{ph}}{I_o} + 1 - \frac{V_{oc}}{I_o R_{sh}}\} \quad \text{.....4.3}$$

and if $R_{sh} \approx \infty$, then

$$V_{oc} \approx \frac{nKT}{q} \ln(\frac{I_{ph}}{I_o} + 1) \quad \text{.....4.4}$$

V_{oc} is determined by the properties of the semiconductor by virtue of its dependence on I_0.

4.1.3. Maximum power output, P_{max}:

I_{max} and V_{max} are the coordinates of the maximum in the P(V) curve.

The maximum power corresponds to the area of the largest rectangle, which can fit inside the I-V curve. There is one particular operating point (V_{max}, I_{max}) that will maximize this power output.

4.1.4. Fill Factor, FF:

It is the ratio of maximum power to the external short and open circuit values.

$$FF = \frac{I_{max} \times V_{max}}{I_{sc} \times V_{oc}} \quad \text{.....4.5}$$

It indicates the deflection of the I-V characteristics from the square like curve and it is therefore dependent on the series and shunt resistance. To obtain high F.F., R_s has to be as small as possible while R_{sh} needs to be as high as possible as shown in figure 4.3 below;

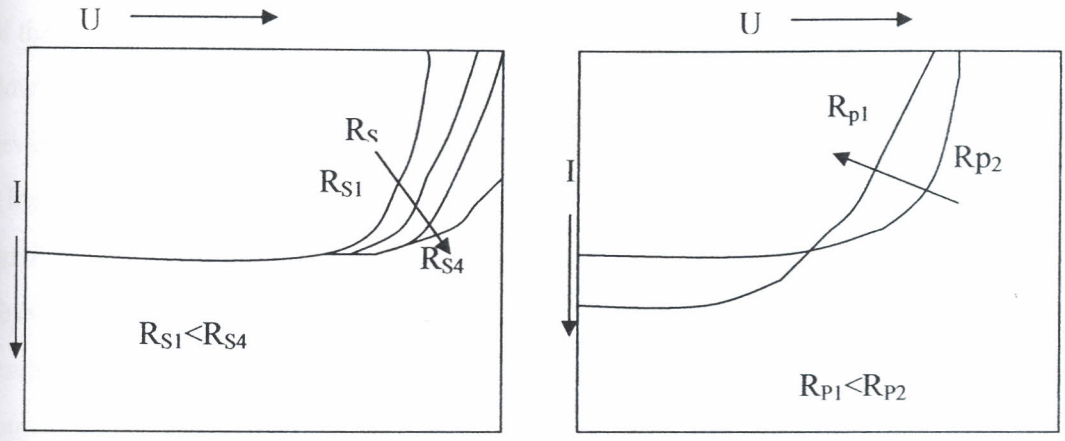

(a) (b)

Fig 4.3 (a) and (b) illustrate the influence of increasing series resistance Rs and decreasing shunt resistance Rsh on the current (I)-Voltage (U) characteristics of a solar cell

Stangl et al. (1998) found that the fill factor has the values in the range of 0.7 to 0.85 and ideally, it is a function only of V_{oc}.

4.1.5. Efficiency (η):

It describes the performance of the solar cell. It is the ratio of the maximum electric power extracted to the radiation power incident on the solar cell surface.

$$\eta = \frac{P\max}{Pin} = \frac{IscVocFF}{Pin} \quad \text{.....4.6}$$

(where P_{in} is the total power in the light incident on the cell).

Losses in the photovoltaic devices are modeled by two resistors, namely, R_s and R_{sh}. There are several physical mechanisms responsible for these resistances.

The major contributor to R_s are the bulk resistance of the semiconductor material making up the cell, the bulk resistance of the metallic contacts and the interconnections and the contact resistance between the metallic contacts and the semiconductor. This means that the R_s models resistive losses such as resistances of the device and electrode and, therefore current traveling through the external circuit loses a portion of its energy to the series resistance.

R_{sh} models all current losses such as current leakages across the p-n junction, around the edges of the cell and exciton recombination or short circuits. This implies that all current that does not flow through the external circuit flows through the shunt resistor. For an ideal photovoltaic device the R_{sh} is infinite and R_s is zero.

Meanwhile, according to Koide et al. (2006), electrochemical impedance spectroscopy (EIS) has been widely used to correlate device structure with a suitable model for the study of the kinetics of electrochemical and photo-electrochemical processes occurring in the DSSCs. EIS results are discussed in terms of equivalent circuits for a semiconductor-electrolyte interface consisting of combination of resistors and capacitors. In this analysis, the three semicircles are attributed to the redox reaction at the platinum counter electrode (Z_1), the electron transfer at the TiO_2 / dye / electrolyte interface (Z_2), and carrier transport by ions within electrolyte (Z_3) as shown in figure 4.4 below;

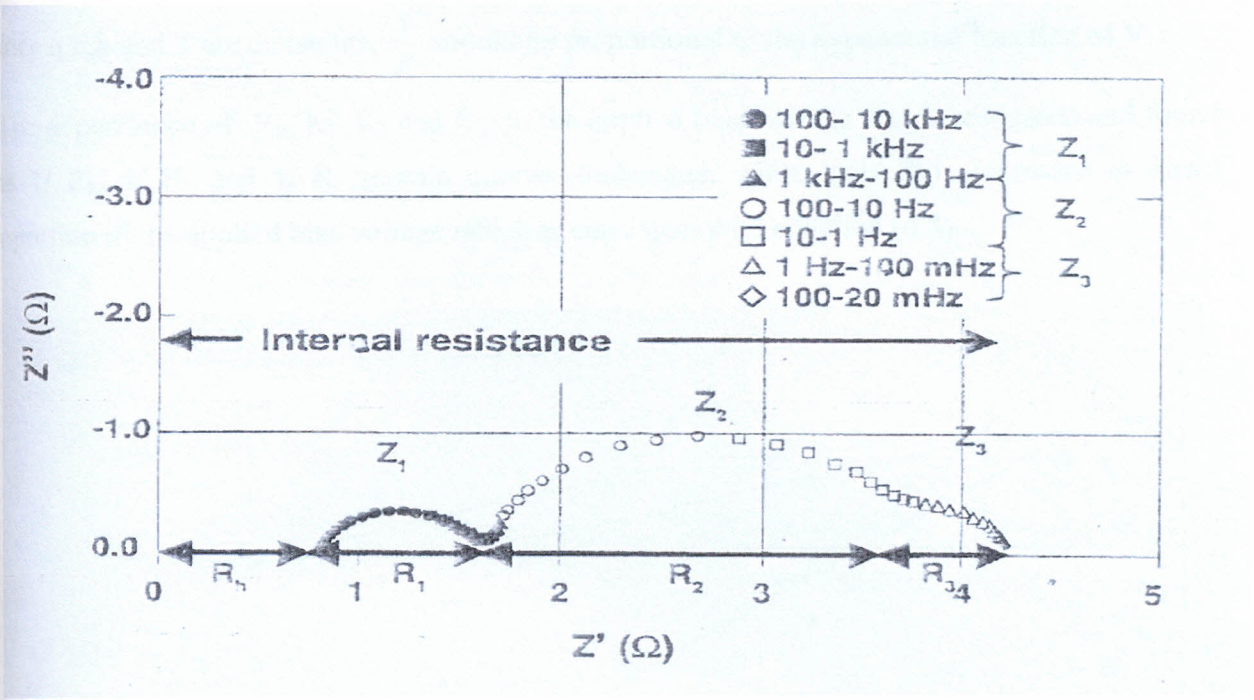

Figure 4.4 Electrical impedance spectrum of a DSSC. The three semicircular shapes are assigned to impedances related to charge transport at the Pt counter electrode (Z_1), at the TiO_2/ dye/ electrolyte interface (Z_2), and the carrier transport by ions within the electrolyte (Z_3), respectively. R_1, R_2 and R_3 are described as the real parts of Z_1, Z_2 and Z_3 respectively. R_h is defined as a resistance in the high-frequency range over 10^6 Hz (Koide 2006).

The resistance elements R_1, R_2 and R_3 are described as the real part of Z_1, Z_2 and Z_3, respectively. It was found that the resistance element R_h in the high frequency range over 1MHz is influenced by the sheet resistance of TCO and the contact resistance between the TCO and TiO_2.

4.2 EQUIVALENT CIRCUIT FOR DSSCs

Solar cells must contain diode like elements though it is difficult to determine which impedance element displays diode like behavior from EIS measurements under open circuit conditions. The I –V characteristics of a diode are given by

$$I=Io\{\exp(\frac{qV}{nkT}) - 1\} \quad \text{.....4.7}$$

where Io, q, V, n, k and T are diode saturation current, elementally charge, voltage, ideality factor, Boltzmann constant and absolute temperature respectively. The resistance R is then described by

$$\frac{1}{R} \propto \exp(\frac{qV}{nkT}) \quad \text{.....4.8}$$

(where $\propto$ is a proportionality symbol)

Since q,n,k and T are constants, $\frac{1}{R}$ should be proportional to the exponential function of V.

The dependence of R_h, R_1, R_2 and R_3 on the applied bias voltage was investigated and found that $1/R_h$, $1/R_1$ and $1/R_3$ remain almost unchanged, while $\ln(1/R_2)$ increases in direct proportion to the applied bias voltage which is consistent with equation (4.8).

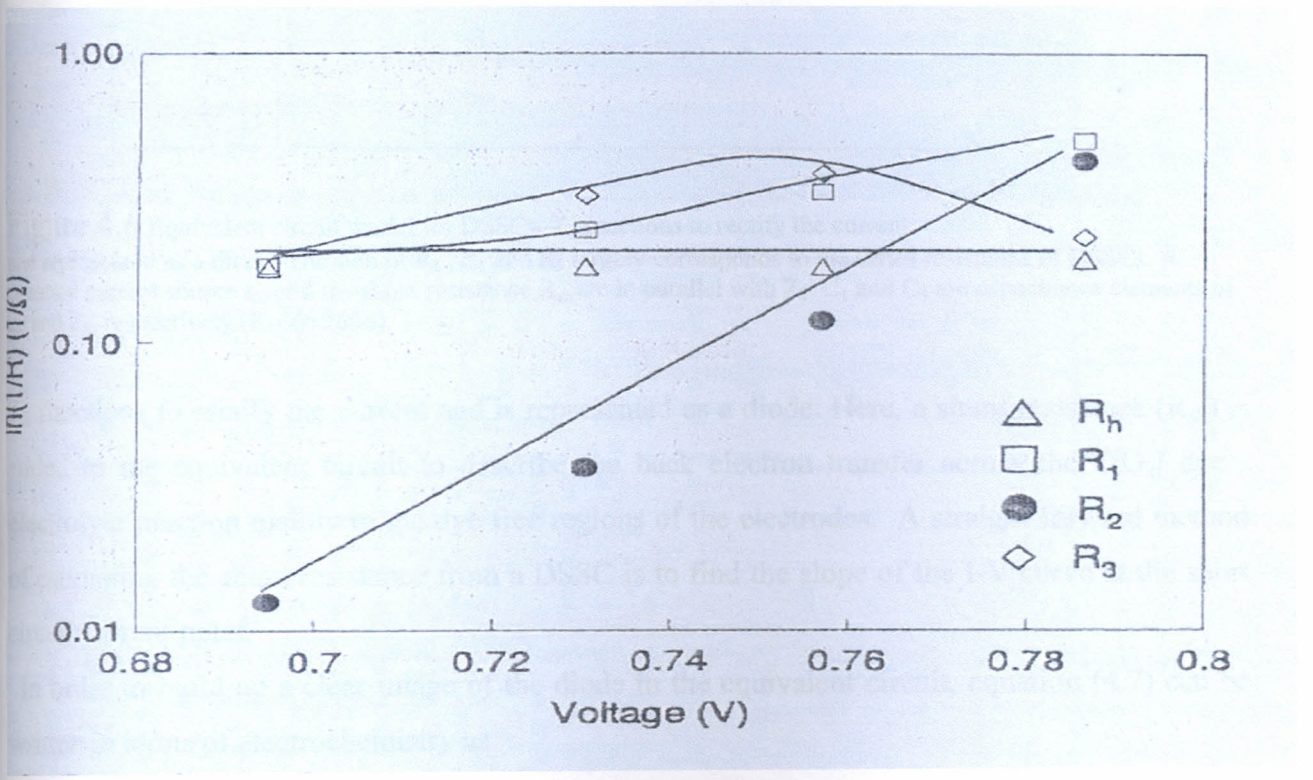

FIGURE 4.5 Dependences of resistances R_h, R_1, R_2 and R_3 on the applied bias voltage. Measurement was carried out under Voc by varying illumination conditions (Koide 2006).

This result suggests that R_2 acts as a diode in DSSCs, while R_h, R_1, and R_3 are series resistance elements.

From experimental analysis by EIS, an equivalent circuit for DSSCs was proposed by Koide et al. (2006) is as shown in figure 4.6:

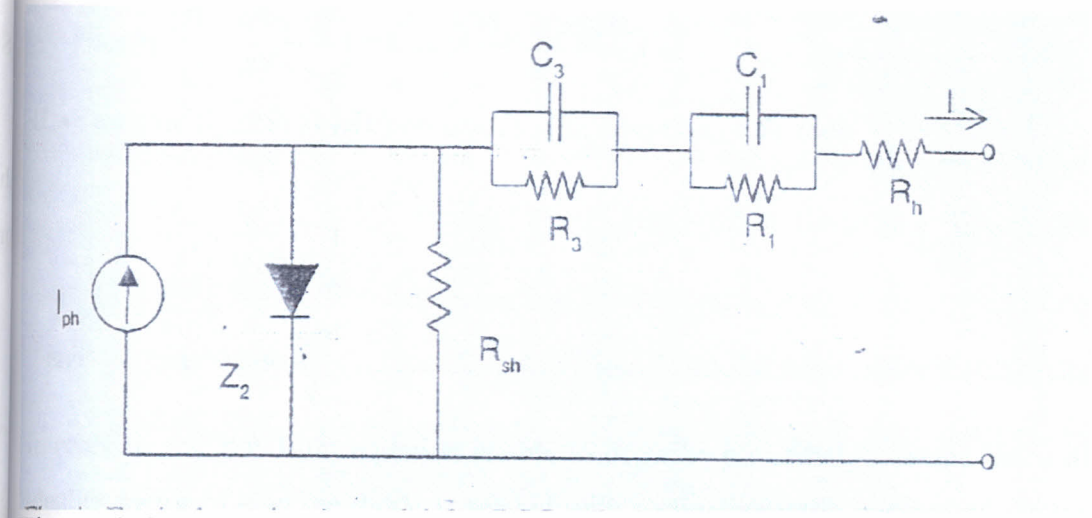

Figure 4.6 Equivalent circuit model for DSSCs. Z_2 functions to rectify the current and represented as a diode. The sum of R_h, R_1 and R_3 largely corresponds to the series resistance of DSSCs. A constant current source I_{ph} and the shunt resistance R_{sh} are in parallel with Z_2. C_1 and C_3 are capacitance elements of Z_1 and Z_3, respectively (Koide 2006).

Z_2 functions to rectify the current and is represented as a diode. Here, a shunt resistance (R_{sh}) is added to the equivalent circuit to describe the back electron transfer across the TiO_2/ dye / electrolyte junction mainly in the dye free regions of the electrodes. A straight forward method of estimating the shunt resistance from a DSSC is to find the slope of the I-V curve at the short circuit current point.

In order to build up a clear image of the diode in the equivalent circuit, equation (4.7) can be written in terms of electrochemistry as

$$i=-i_o\{\exp(\frac{-\alpha mFE}{RT}) - \exp[\frac{(1-\alpha)mFE}{RT}]\} \quad \text{.....4.9}$$

The Butler-Volmer equation (4.9) is well known as the Faradaic current for the electrode interface reaction (where i_o is exchange current, α the transfer coefficient and has a range of $0<\alpha<1$ which is one of the kinetic parameters of the electrode reaction, m is a stoichiometric number of electrons involved in the electrode reaction, F the Faraday constant which equals q times the Avogadro constant, E is the electric potential at the electrode, and R is the gas constant which is defined as k times Avogadro constant). Since electric potential E is much larger than (RT/α mF) under DSSC operational conditions, equation (4.9) according to Koide et al. (2006) can be simplified to a Tafel equation as

$$i=i_o \exp(\frac{(1-\alpha)mFE}{RT}) = I_o \exp(\frac{(1-\alpha)mqE}{kT}) \quad \text{.....4.10}$$

If we assume equation (4.10) coincides with equation (4.7), then

$$(1-\alpha)m = \frac{1}{n} \quad \text{.....4.11}$$

and $$E=V>>\frac{nkT}{q} \quad \text{.....4.12}$$

In other words, the Tafel equation is able to describe a rectifiable device like a diode, while the ideality factor of n in the diode is related with a stiochiometric number of electrons involved in the electrode reaction, m, and the transfer coefficient, α.

Comparison of the equivalent circuit for DSSCs (fig. 4.6) and conventional p-n junction solar cells (fig. 4.1) shows that there is a difference only in series resistance. In the case of DSSCs, series resistance is paralleled with two large capacitance elements, C_1 of the order of 10 μ F/cm^2 and C_3 of the order of 1F/cm^2.

These capacitance elements bring a large time constant which causes slow response to applied bias in measurement such that correct measurement should be carried out with a prolonged delay time for measuring the current-voltage characteristics based on the equivalent circuit. However, capacitance elements can be omitted since solar cells are generally operated under direct current conditions. Consequently, R_s can be described as

$$R_s = R_h + R_1 + R_3 \quad \text{.....4.7}$$

Under direct current conditions, Koide et al. (2006) found that, the equivalent circuit for DSSCs is similar to that for the conventional solar cells, although the mechanism is very different. This suggests that the accumulated experience gained through the development of high efficiency conventional solar cells can be applied to DSSCs.

CHAPTER 5

EFFECT OF TEMPERATURE ON DSSCs

5.1 TEMPERATURE DEPENDENCE OF THE ENERGY GAP

Streetman (2004) found that the energy band gap of the semiconductors tends to decrease as the temperature is increased. This behaviour can be understood if one considers that the inter-atomic spacing increases when the amplitude of the atomic vibrations increases due to the increased thermal energy. This effect is quantified by the linear expansion coefficient of a material. An increased inter-atomic spacing decreases the average potential seen by the electrons in the material, which in turn reduces the size of the energy band gap. A direct modulation of the inter-atomic distance such as by applying (tensile) compression also causes an increase (decrease) of the band gap.

The temperature dependence of the energy band gap, E_g, has been experimentally determined yielding the following expression for E_g as a function of the temperature, T (Millman and Halkias, 1991).

$$E_g(T) = E_g(0) - \frac{\alpha T^2}{T + \beta} \quad \text{.....5.1}$$

where $E_g(0)$, α and β are constants and Eg(0) represents energy gap at 0K.

The dye-cell constitute, in addition to the active semiconductor electrode, an organic dye and a liquid electrolyte. Redox processes at interfaces have different time scales. The charge transfer at the TiO_2 / dye interface is higher than that of dye / electrolyte or that of electrolyte / electrode inter-face. The diffusion limited electrical conduction mechanism in the cell can be influenced by the operating temperature.

The opto-electronic properties of the cell depend on the factors like ambient temperature and the time constants of the redox processes at the cell interfaces. This implies that operating temperature is an important parameter which influences the opto-electronic characteristic of this type of cell, especially when the cell utilizes a liquid medium as dye and electrolyte.

The temperature response of the opto-electronic properties such as the voltage, current, photovoltaic power, efficiency, fill factor, etc, of dye sensitized nano-crystalline TiO_2 solar cell

is similar to a solid state photovoltaic cell where the current increases while voltage, power, efficiency, fill factor decrease at temperatures far away (high or low) from ambient temperature.

5.2 MAXIMUM USEFUL TEMPERATURE OF A SEMICONDUCTOR DEVICE.

When the working temperature of an extrinsic semiconductor is increased, the thermally generated carrier pairs also increases proportionally to a level where they are either equal or even greater than those contributed by impurities whose number is fixed.

At this juncture, the semiconductor loses its extrinsic nature and becomes intrinsic where the number of holes equals the number of electrons. Since the semiconductor is based on n-type, p-type or n-type in some region and p- type in others, any semiconductor device has its maximum operation extrinsic temperature, T_{max}, of which for better desirable output one should operate such a device far below such value.

For the case of an n-type, we get T_{max} by taking the condition that $n_i \approx N_D$. Bar-Lev (1993) proved that by introducing impurities to the semiconductors does not change the basic approach from the result found for n and p in the intrinsic case. What changes is only the form of the neutrality condition which results to the shifting of E_F. In the extrinsic equilibrium conditions $\bar{n} \neq \bar{p}$ we know that

$$\bar{n} = N_C \exp(-\frac{E_C - E_F}{kT}) \quad \text{.....5.2}$$

and $$\bar{p} = N_V \exp(-\frac{E_F - E_V}{kT}) \quad \text{.....5.3}$$

and on getting the product $\bar{n}\bar{p}$ we get

$$\bar{n}\bar{p} = N_C N_V \exp(\frac{-(E_C - E_V)}{kT}) \quad \text{.....5.4}$$

or $$\bar{n}\bar{p} = N_C N_V \exp(\frac{-E_g}{kT}) = n_i^2 \text{ where } E_g = E_C - E_V$$

$I_0 = AT^m \exp\left(\frac{-E_{go}}{kT}\right)$ 5.10

(where A, m, k and E_{go} are constants)

and taking the natural logarithm of both sides of equation (5.10) we get

$\ln I_0 = \ln A + m \ln T - \frac{E_{go}}{kT}$ 5.11

Differentiating (5.11) w.r.t. T yields (Millman and Halkias,1991)

$$\frac{d(\ln I_0)}{dT} = m\frac{d(\ln T)}{dT} + \frac{E_{go}}{kT^2} \quad \text{or}$$

$$\frac{dI_0}{I_0 dT} = \frac{m}{T} + \frac{E_{go}}{kT^2} \quad \text{.....5.12}$$

Taking the natural logarithm of (5.9) we get

$\ln I_{ph} = \ln I_0 + \frac{qV_{OC}}{nkT}$ 5.13

Differentiating (5.13) w.r.t. T yields

$$\frac{dI_{ph}}{I_{ph}dT} = \frac{dI_0}{I_0 dT} + \frac{q}{nkT}\frac{dV_{OC}}{dT} - \frac{qVoc}{nkT^2} \quad \text{.....5.15}$$

Substituting (5.12) into (5.15), we get

$$\frac{dI_{ph}}{I_{ph}dT} = \frac{m}{T} + \frac{E_{go}}{kT^2} + \frac{q}{nkT}\frac{dV_{OC}}{dT} - \frac{qVoc}{nkT^2} \quad \text{.....5.14}$$

Since I_{ph} is not a strong temperature dependent, equation (5.14) can be re-written as

$$\frac{q}{nkT}\frac{dV_{OC}}{dT} = \frac{qVoc}{nkT^2} - \frac{m}{T} - \frac{E_{go}}{kT^2} \quad \text{or}$$

$$\frac{dV_{OC}}{dT} = \frac{V_{OC}}{T} - \frac{nkm}{q} - \frac{nE_{go}}{qT} \quad \text{or}$$

$qT\ dV_{OC} + (nE_{go} + nkm\,T - q\,V_{OC})\,dT = 0$.....5.15

From Riley et al.(1998) this is a first order first degree differential equation which can be solved as follows;

let $qT = A$.....5.16

$nE_{go} + nkm\,T - q\,Voc = B$.....5.17

$$\frac{dA}{dT} = q \text{.....5.18}$$

$$\frac{dB}{dV_{OC}} = -q \text{.....5.19}$$

$$\frac{1}{A}\left(\frac{dB}{dV_{OC}} - \frac{dA}{dT}\right) = \frac{1}{qT}(-q - q) = \frac{-2q}{qT} = \frac{-2}{T} \text{.....5.20}$$

Integrating factor (I. F.) $= e^{-2\int\frac{1}{T}dT} = e^{-2\ln T} = e^{\ln T^{-2}} = \frac{1}{T^2}$.....5.21

Multiplying (5.15) by I.F. we get

$$\frac{q}{T}\,dV_{OC} + \left(\frac{nE_{go}}{T^2} + \frac{nkm}{T} - \frac{qV_{OC}}{T^2}\right)dT = 0 \text{.....5.22}$$

Note that now equation (5.22) is exact, that is

$$\frac{dA}{dT} = -\frac{q}{T^2} = \frac{dB}{dVoc}$$

And it can easily be shown that

$$U(T, V_{OC}) = \int B dT + F(V_{OC})$$

$$= \int \left(\frac{nE_{go}}{T^2} + \frac{nkm}{T} - \frac{qV_{OC}}{T^2}\right) dT + F(V_{OC})$$

$$U(T, V_{OC}) = -\frac{nE_{go}}{T} + \frac{qV_{OC}}{T} + nkm \ln T + F(V_{OC}) = C_1 \quad \text{.....5.23}$$

Differentiating (5.23) w.r.t. Voc and equating the result to A(T, V_{OC}), we get

$$\frac{q}{T} = \frac{q}{T} + \frac{dF(V_{OC})}{dV_{OC}} \quad \text{or.....5.24}$$

$$\frac{dF(V_{OC})}{dV_{OC}} = 0 \quad \text{.....5.25}$$

$$dF(V_{OC}) = 0 \quad \text{.....5.26}$$

Integrating yields

$$F(V_{OC}) = C_2 \quad \text{.....5.27}$$

Subtracting (5.27) from (5.23), we get

$$nkm \ln T + \frac{qV_{OC}}{T} - \frac{nE_{go}}{T} = C_2 - C_1 = C \quad \text{.....5.28}$$

which can be solved from the following initial conditions obtained from Waita's Ph.D thesis (2008).

n=2.08 $E_{go} = 3.2 \times 1.6O2 \times 10^{-19}$J

k= 1.38×10^{-23} $V_{OC} = 0.63$V

m=3 T=298K

thus, C=(n*k*m*log(T))+((q*Voc)/T)-((n*Ego)/T).....5.29

After getting C, we can express V_{OC} explicitly in terms of T. That is

$$VOC = \frac{nE_{go}}{T} - nkm \ln + C \quad \text{.....5.30}$$

Where VOC has been adopted to denote the open circuit voltage which is a variable while Voc is taken as a constant to assist us in computing the value of constant, C.

$$VOC = \frac{nE_{go}}{T} - nkm \ln T + (n*k*m*\log(T)) + ((q*Voc)/T) - ((n*Ego)/T) \quad \text{.....5.31}$$

(For computer simulation, see appendix 1)

Using equation (5.31) the curve of open circuit voltage,Voc, versus Temperature, T, is plotted as shown in figure 5.2, it depicts a decline in voltage as the temperature is increased above the room temperature.

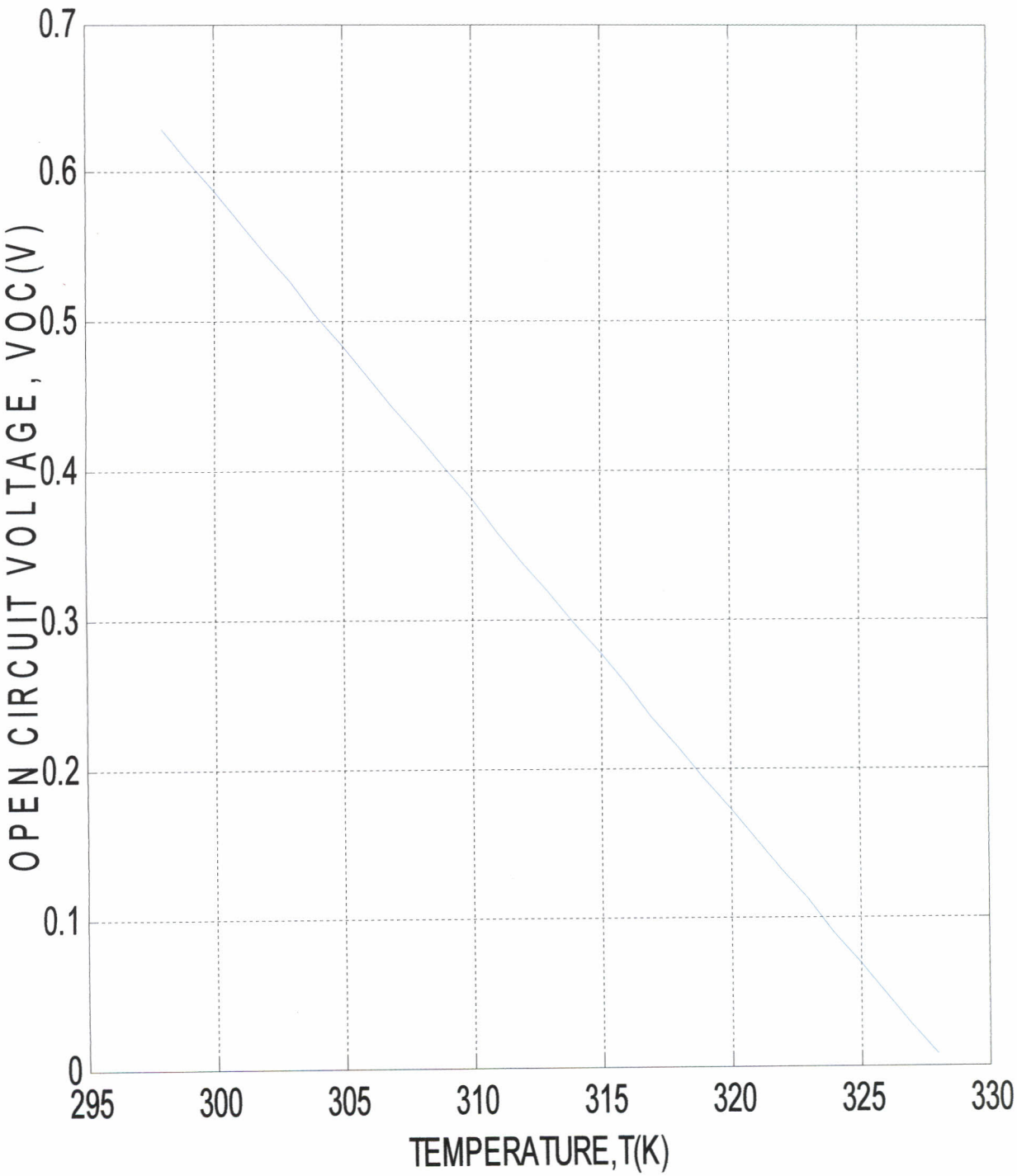

Figure 5.1 Variation of open circuit voltage (V_{OC}) with the temperature (T).

5.4 VARIATION OF SHORT CIRCUIT CURRENT (I_{sc}) WITH THE TEMPERATURE (T).

From the Schottky equation (5.7), when V=0, $I = I_{sc}$ which reduces equation (5.7) to;

$$I_{sc} = I_{ph} - I_o\{\exp(\frac{qI_{sc}R_s}{nkT}) - 1\} - \frac{I_{sc}R_s}{R_{sh}} \quad \text{.....5.32}$$

Further, neglecting -1 in comparison with the exponent, equation (5.32) above reduces to;

$$I_{sc} = I_{ph} - I_o \exp(\frac{qI_{sc}R_s}{nkT}) - \frac{I_{sc}R_s}{R_{sh}} \quad \text{.....5.33}$$

which is a non linear equation and cannot be solved by separation of variables methods. Such an equation can only be solved using iteration method of a very powerful computer software such as Matlab since I_{sc} cannot be expressed explicitly in terms of T.

By using $I_{ph}, I_0, I_{sc}, q, n, k, T, R_s$ and R_{sh} as simulation parameters of a specific DSSC, Waita et al. (2008) using TiO_2 film of thickness 3.0 μm, solar irradiation of 1000W/m^2, active area of 0.785 cm^2 and at a temperature (T) of 25^{O}C (298K) got the following results;

$I_0 = 0.37\times10^{-6}$ A $\qquad$ $I_{ph} = 2.62\times10^{-3}$ A

$R_s = 19.77\ \Omega$ $\qquad$ $R_{sh} = 10086.14\times10^3\ \Omega$

n=2.08 $\qquad$ $V_{oc} = 0.63V$

Using the Matlab computer software, shown in appendix 2, with temperature being taken within the range of 298K to 328K and with the I_{sc} taken within the range of 8.7916×10^{-4} A to 8.7917×10^{-4} A the following simulation curve was obtained using equation 5.22 as shown in figure 5.2. The curve shows that there is a slight increase in current as the temperature is increased above the room temperature.

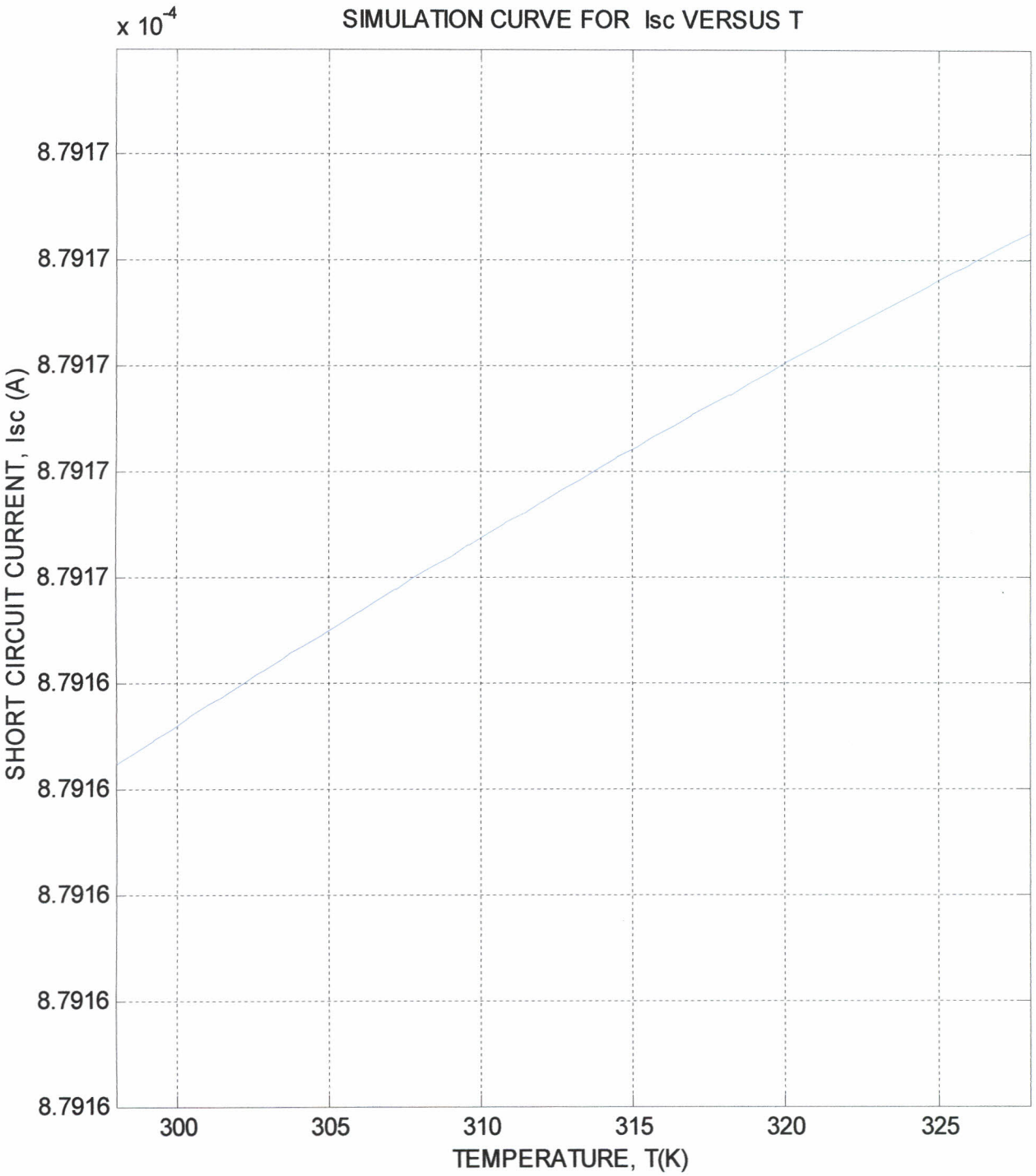

Figure 5.2 Variation of short circuit current, I_{sc} (A) with temperature, T (K) within the range of $298K \leq T \leq 328K$ for a DSSC.

CHAPTER 6

CONCLUSION AND SUGGESTION FOR FURTHER WORK

The outcome of my project after developing relevant equations of some of the optoelectronic properties of DSSCs and after computer simulation, I have found out that the open circuit voltage (V_{oc}) reduces with the increase in temperature above the ambient temperature (298 K) while the short circuit current (I_{sc}) increases only slightly with the increase in temperature within the same range. This is in agreement with what has already been experimentally proved by Musembi et al.(2008).

Since the efficiency, maximum power output and the fill factor depend on V_{oc}, it is therefore important to design the solar cell modules in such a way that their surface structures reflect away most of the radiant heat energy for maximal output. Also the roof tops where the solar modules are mounted should be made of material that is a poor conductor of radiant heat since good conductors are also good emitters of heat. The solar modules should be raised slightly from the roof tops to minimize the radiant heat from the surface that supports them.

I would suggest further research on how;

1. The fill factor, maximum power output, series resistance and shunt resistance individually varies with temperature.
2. I would suggest also further research on how every component of the DSSC is affected when the temperature varies so that one common I-V curve can be simulated which can provide all parameters of a DSSC at a given temperature.
3. To compare the short circuit current versus temperature curve that I got, I would suggest a similar simulation curve to be drawn using short circuit current equation developed using Lambert W function.

APPENDIX 1

DATA ANALYSIS AND COMPUTER SIMULATION

To get started, select "MATLAB Help" from the Help menu.

```
>> n=2.08;
>> k=1.38*10^-23;
>> m=3;
>> q=1.62*10^-19;
>> Voc=0.63;                % Voc here is a fixed value so as to determine constant,C.
>> Ego=3.2*1.62*10^-19;     %Ego is the TiO2 (anatase) at 0K
>> T1= 298;                 % T1 has been chosen to be the room temperature
>> C=(n*k*m*log(T1))+((q*Voc)/T1)-((n*Ego)/T1)

C =

 -2.7180e-021
>> T2=298:1:328
T2 =
  Columns 1 through 16
   298   299   300   301   302   303   304   305   306   307   308   309   310   311   312   313
  Columns 17 through 31
   314   315   316   317   318   319   320   321   322   323   324   325   326   327   328

>> VOC=(((n*Ego)/q)-((n*k*m*(T2).*log(T2))/q)+(T2*(n*k*m*log (T1)+(q*Voc)/T1-
(n*Ego)/T1))/q)
VOC =

  Columns 1 through 16

   0.6800   0.6594   0.6388   0.6182   0.5976   0.5770   0.5564   0.5358   0.5152   0.4946
0.4740   0.4534   0.4328   0.4122   0.3915   0.3709
```

Columns 17 through 31

0.3503 0.3297 0.3091 0.2884 0.2678 0.2472 0.2266 0.2059 0.1853 0.1647 0.1440 0.1234 0.1027 0.0821 0.0615

```
>> plot(T2,VOC)
>> hold on
>> xlabel('TEMPERATURE,T(K)');
>> title('COMPUTER SIMULATION CURVE FOR OPEN CIRCUIT VOLTAGE VERSUS TEMPERATURE');
>> ylabel('OPEN CIRCUIT VOLTAGE, VOC(V)');
>> grid on
>> hold off
```

APPENDIX 2

DATA ANALYSIS AND COMPUTER SIMULATION

$$I_{sc} = I_{ph} - I_o \exp(\frac{qI_{sc}R_s}{nkT}) - \frac{I_{sc}R_s}{R_{sh}}$$

I_0 =0.37×10^{-6} A

I_{ph} =2.62×10^{-3} A

R_s =19.77 Ω

R_{sh} =10086.14×10^3 Ω

n=2.08

V_{oc} =0.63 V

To get started, select "MATLAB Help" from the Help menu.

```
>>f=inline('I+((19.97.*I)/10086.14*10^3)+0.37*10^-6*(exp((1.6*10^-
19*19.77.*I)/(2.08*1.38*10^-23.*T))-1)-2.62*10^-3','T','I');
>> implot (f,[298 328 0.00087916  0.00087917])
>> hold on
>> xlabel ('TEMPERATURE, T(K)');
>> ylabel ('SHORT CIRCUIT CURRENT, Isc (A)');
>> title ('SIMULATION CURVE FOR  Isc VERSUS T');
>> grid on
>> hold off
```

LIST OF REFERENCES

Bar-Lev A. (1993). *Semiconductor and Electronic Devices*, Prentice Hall International (UK) Ltd, 21-112.

BP,(2003).

BGR,(2002).

Granqvist, C. G., (2007), Transparent Conductor as Solar Energy Materials: A Panoramic Review, *Solar Energy Materials and Solar Cells*, **91**, 1529-1597.

Green M. A., (1992). *Solar Cells*: *Operating Principles*, The University of New South Walls, Kensington, 4-92.

G'omezle'on, M.M., (2001). *Photo-electrochemical and Physical Properties of Sputer Deposited Titanium Oxide Electrodes*, Faculty of Science –Lima, 23-25.

International Energy Agency, (2002), *Trends in Photovoltaic Applications in Selected IEA Countries Between 1992 and 2001 in Photovoltaic Power Programme*, Report IEA PVPSTI-11.

Kalyanasundaram, K.M. Gratzel, (1998), Application of functionalized transition metal complexes in photonic and opto-electronic device, *Coordination Chemistry Reviews*, **77**, 356-366.

Koide, K., A. Islm, Y. Chiba, L. Han (2006). Improvement of Efficiency of Dye-Sensitized Solar Cells Based on Analysis of Equivalent Circuit, *Journal of Photochemistry and Photobiology A: Chemistry*,**182**, 286-289.

Millman, J., C.C. Halkias, (1991). *Integrated Electronics*, TataMcGraw-Hill, 19-752.

Riley, K. F., M.P. Hobson, S. J. Bence, (1998), *Mathematical Methods for Physics and Engineering*, Sheck Wah Tong, Hong Kong, 377-380.

Musembi. R. J., M. Rusu, J. M. Mwabora, B.O. Aduda, K. Fostiropoulos, M. C. Lux-steiner, (2008), Intensity and Temperature Dependent Characterization of ETA Solar cell, *Physica Status Solidni(a),* **205**, (7),1713-1718.

Stangl, R., J. Ferber , J. Luther, (1998). Modeling of the DSSC, *Solar energy materials and solar cells*, **54** ,255 - 256.

Streetman B.G., S. Banerjee, (2004). *Solid State Electronic Devices*, Prentice Hall of India.

Waita, S. M, (2008), Ph D Thesis entitled '*Dye Sensitized Solar Cells Fabricated From Obliquely Sputtered Nanoporous TiO_2. Thin Film: Characterization, Electron Transport and Life Time Studies*', University of Nairobi.

Wanzella, M. C., R.N.C. Alves, J.V.F. Neto, W.A.S. Fonseca (2004). Current Control Loop for Tracking of Maximum Power Point Supplied for Photovoltaic Array, *IEEE Transactions on Instrumentation and Measurement*, **53** (4), 1304-1310.